

Article

## Hip to be square: oxetanes as design elements to alter metabolic pathways

Francesca Toselli, Marlene Fredenwall, Peder Svensson, Xue-Qing Li, Anders Johansson, Lars Weidolf, and Martin A Hayes

*J. Med. Chem.*, **Just Accepted Manuscript** • DOI: 10.1021/acs.jmedchem.9b00030 • Publication Date (Web): 16 Jul 2019

Downloaded from [pubs.acs.org](https://pubs.acs.org) on July 17, 2019

### Just Accepted

“Just Accepted” manuscripts have been peer-reviewed and accepted for publication. They are posted online prior to technical editing, formatting for publication and author proofing. The American Chemical Society provides “Just Accepted” as a service to the research community to expedite the dissemination of scientific material as soon as possible after acceptance. “Just Accepted” manuscripts appear in full in PDF format accompanied by an HTML abstract. “Just Accepted” manuscripts have been fully peer reviewed, but should not be considered the official version of record. They are citable by the Digital Object Identifier (DOI®). “Just Accepted” is an optional service offered to authors. Therefore, the “Just Accepted” Web site may not include all articles that will be published in the journal. After a manuscript is technically edited and formatted, it will be removed from the “Just Accepted” Web site and published as an ASAP article. Note that technical editing may introduce minor changes to the manuscript text and/or graphics which could affect content, and all legal disclaimers and ethical guidelines that apply to the journal pertain. ACS cannot be held responsible for errors or consequences arising from the use of information contained in these “Just Accepted” manuscripts.

# Hip to be square: oxetanes as design elements to alter metabolic pathways

*Francesca Toselli<sup>†,§</sup>, Marlene Fredenwall<sup>†</sup>, Peder Svensson<sup>‡</sup>, Xue-Qing Li<sup>†</sup>, Anders Johansson<sup>†</sup>, Lars Weidolf<sup>†</sup> and Martin A. Hayes<sup>†,\*</sup>*

<sup>†</sup>Cardiovascular, Renal and Metabolism, Innovative Medicines and Early Development Biotech Unit, AstraZeneca, Pepparedsleden 1, Mölndal, 431 83, Sweden

<sup>‡</sup>Integrative Research Laboratories, Arvid Wallgrens Backe 20, Gothenburg, 413 46, Sweden.

## KEYWORDS

Oxetane, epoxide hydrolase, metabolic clearance, drug design, spirocycles

## ABSTRACT

Oxetane-containing ring systems are increasingly used in medicinal chemistry programs to modulate drug-like properties. We have shown previously that oxetanes are hydrolyzed to diols by human microsomal epoxide hydrolase (mEH). Mapping the enzymes which contribute to drug metabolism is important, since an exaggerated dependence on one specific isoenzyme increases the risk of drug-drug interactions with co-administered drugs. Herein we illustrate that mEH-catalyzed hydrolysis is an important metabolic pathway for a set of more structurally diverse oxetanes and the degree of hydrolysis is modulated by minor structural modification. A

1  
2  
3 homology model based on the *Bombyx mori* EH crystal structure was used to rationalize  
4 substrate binding. This study shows that oxetanes can be used as drug design elements for  
5 directing metabolic clearance *via* mEH, thus potentially decreasing the dependence on  
6 cytochromes P450. Metabolism by mEH should be assessed early in the design process to  
7 understand the complete metabolic fate of oxetane-containing compounds and further study is  
8 required to allow accurate PK prediction of its substrates.  
9  
10  
11  
12  
13  
14  
15  
16  
17

## 18 INTRODUCTION

19  
20  
21

22 Early work in drug discovery programs aims at optimizing a host of compound properties like  
23 pharmacological potency, off-target profile and pharmacokinetic properties, including metabolic  
24 stability. All these properties are important for the prediction of dose and dosing frequency, to  
25 reach the desired target engagement and efficacy in clinical trials. However, not only is it  
26 essential to achieve sufficient metabolic stability of a clinical candidate, but also to understand  
27 the metabolic pathways and the enzymes involved in the metabolism of the molecule.  
28  
29  
30  
31  
32  
33  
34  
35

36 The majority of marketed drugs depend on cytochrome P450 (CYP) isoenzymes for their  
37 metabolic clearance.<sup>1,2</sup> This is a potential concern in drug discovery programs, as there is a risk  
38 of interaction between drugs that are metabolized to a large extent by the same CYP isoenzyme.  
39 Such interactions can lead to elevated drug plasma levels and unwanted side effects for patients  
40 taking several medications. This phenomenon is known as drug-drug interactions (DDI) and any  
41 drug entering clinical trials must be carefully evaluated and monitored from a DDI perspective. It  
42 is therefore desirable to optimize a lead series to minimize the risk of DDI. Designing away from  
43 dependence on CYP-mediated metabolism is however not trivial and may result in switching of  
44 the metabolism to non-CYP metabolizing enzymes e.g. aldehyde oxidase.<sup>3,4</sup> A downside of  
45  
46  
47  
48  
49  
50  
51  
52  
53  
54  
55  
56  
57  
58  
59  
60

1  
2  
3 directing metabolism to less-studied enzymes is that our understanding of their biology is not as  
4  
5 mature as that for CYPs and can lead to problems in human PK prediction.<sup>5-8</sup>  
6

7  
8 A functional group increasingly used for improving drug-like properties in medicinal  
9  
10 chemistry is the oxetane ring.<sup>9,10</sup> It has been used as a mimic for carbonyl groups e.g. in  
11  
12 enzymatically-stable peptides<sup>11</sup> or as a more hydrophilic replacement of a gem dimethyl  
13  
14 group.<sup>12,13</sup> Oxetane-containing spirocyclic ring systems have proven to be versatile building  
15  
16 blocks, by improving the physicochemical properties and providing more favorable  
17  
18 pharmacokinetic profiles of a lead series.<sup>14-20</sup>  
19  
20

21  
22 Recently, the introduction of the spirocyclic oxetanylazetidiny moiety led to discovery of the  
23  
24 clinical candidate AZD1979 (**1**), a melanin-concentrating hormone receptor 1 antagonist  
25  
26 designed for the treatment of obesity-related disorders.<sup>21</sup> Careful characterization of the  
27  
28 enzymology of its metabolism revealed that the oxetane moiety undergoes ring-opening in liver  
29  
30 fractions *via* an unusual non-oxidative metabolic route, *i.e.* hydrolysis by human microsomal  
31  
32 epoxide hydrolase (mEH; EC 3.2.2.9).<sup>22</sup> This was the first example of a non-epoxide substrate  
33  
34 for this important drug-metabolizing enzyme, which was previously known to only catalyze  
35  
36 hydrolytic opening of epoxide-containing drug metabolites formed *via* Phase I oxidation.<sup>23,24</sup> A  
37  
38 subsequent study on simple oxetanes from the same chemical series along with truncated  
39  
40 analogues revealed that oxetane hydrolysis by human mEH was not limited to **1**.<sup>25</sup> Thus, there is  
41  
42 evidence that these strained rings constitute a new class of substrates for mEH. This observation  
43  
44 has recently been recognized by the International Union of Biochemistry and Molecular Biology  
45  
46 with a change in the definition of mEH, now known as microsomal oxirane/oxetane hydrolase.<sup>26</sup>  
47  
48 The rate of hydrolysis can be fine-tuned by structural elements in the vicinity of the oxetane.<sup>25</sup>  
49  
50  
51  
52 This implies that oxetane-containing building blocks could be used as design tools to open up an  
53  
54  
55  
56  
57  
58  
59  
60

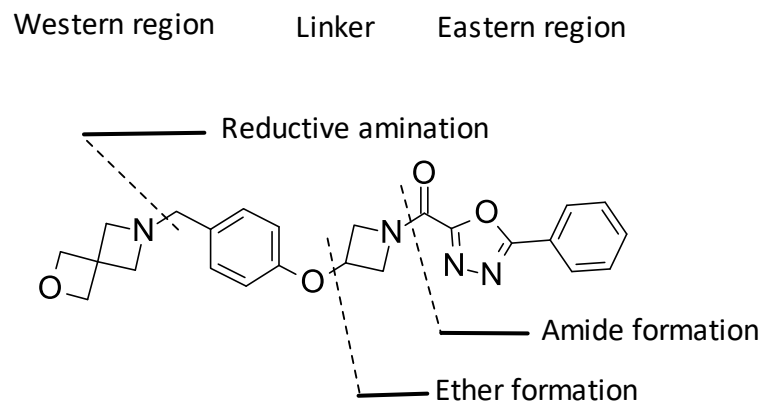
1  
2  
3 alternative metabolic clearance pathway and, potentially, to decrease the dependence on CYP-  
4 mediated metabolic clearance.  
5  
6

7 The primary aim of the current study was to investigate hydrolytic ring-opening by mEH on a  
8 more diverse set of oxetane-containing spirocycles related to **1**, broadening our understanding of  
9 the structure-activity relationship (SAR) of spirocyclic and bicyclic motifs. Secondly, an  
10 additional set of simple oxetanes from an entirely different chemical series were investigated, to  
11 understand the generality of oxetane hydrolysis by human mEH. Finally, due to the lack of a  
12 crystal structure of human mEH, a homology model was built to better understand the SAR of  
13 oxetane hydrolysis and to rationalize substrate binding. The findings presented here further  
14 emphasize how the hydrolysis of simple and spirocyclic oxetanes by mEH is affected by subtle  
15 structural modifications. Our results also indicate that metabolism can be directed towards mEH,  
16 thus decreasing dependence on oxidative metabolism by CYP enzymes though caution should be  
17 exercised if non-CYP enzymes are considered as major routes of clearance since PK predictions  
18 may be challenging.<sup>5-8</sup>  
19  
20  
21  
22  
23  
24  
25  
26  
27  
28  
29  
30  
31  
32  
33  
34  
35  
36  
37

## 38 RESULTS AND DISCUSSION

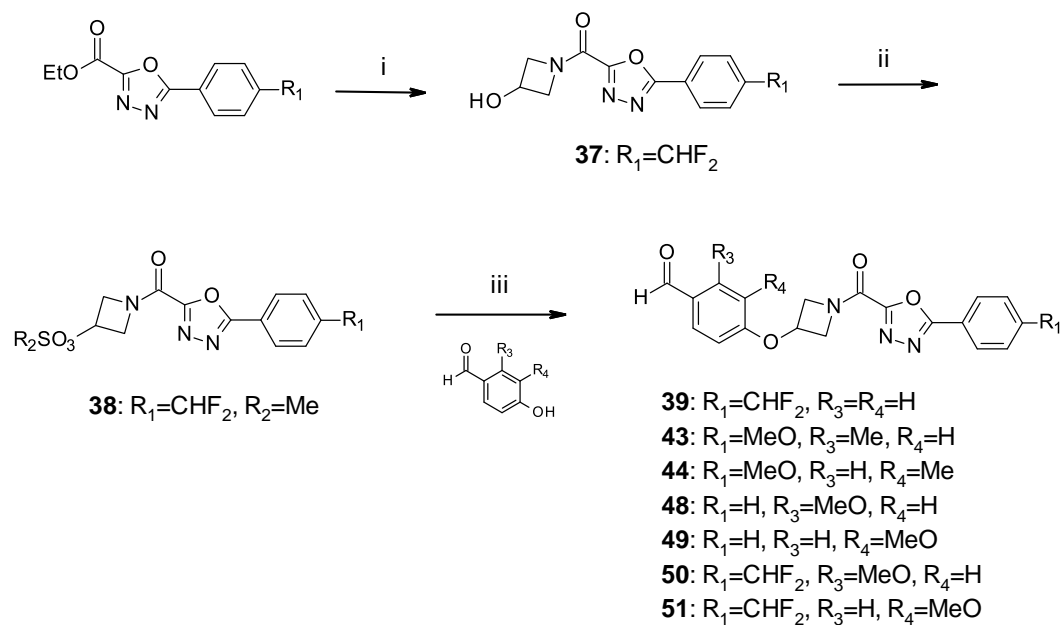
39  
40  
41

42 The compounds studied consisted of different ring-size combinations of bicyclic *O*- and *N*-  
43 containing heterocycles with an emphasis on spirocyclic oxetanes (compounds **1-11**, Table 1),  
44 (compounds **16-23**, Table 2), (compounds **24-27**, Table 3) and a set of oxetane-substituted  
45 pyrimidines (compounds **29-34**, Table 4). The bicyclic oxetanes compounds were prepared  
46 according to three different synthetic strategies (Figure 1). The majority of the compounds were  
47 synthesized in a linear manner starting with the preparation of the eastern region esters.  
48  
49  
50  
51  
52  
53  
54  
55  
56  
57  
58  
59  
60

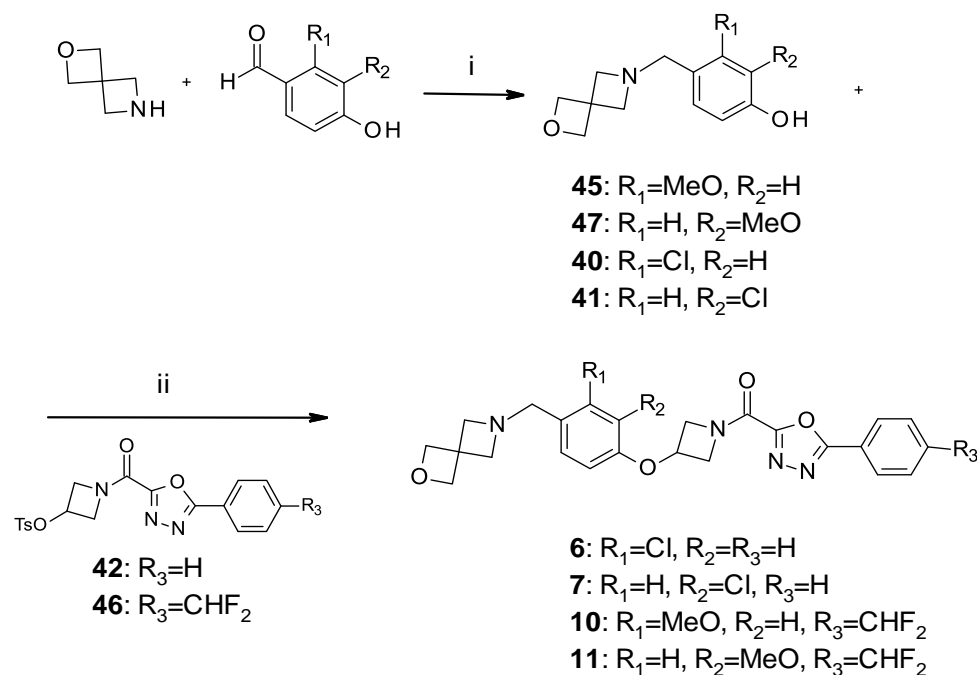


**Figure 1.** Synthetic routes to oxetane heterocycles.

The final step following this strategy was a reductive amination between a benzylic aldehyde precursor and an oxetane-containing amine. This strategy allowed for preparation of several bicyclic oxetane amines from a common building block. A second strategy was amide formation between an azetidine precursor and an eastern region ester, which, of course, is complementary to the reductive amination strategy and allows for variation of the eastern region on a common western region building block. The third and most convergent synthetic strategy was to form the central ether bond as the last step. Both amide and ether formation were less commonly used for preparation of target compounds, but they were useful for preparing larger batches when atom economy is more important. It should be mentioned that ether formation appears to be more substrate dependent and in some cases quite poor yields were observed. Synthetic routes for the preparation of building blocks and target compounds are shown in **Schemes 1** and **2**. Several of the building blocks have been reported previously<sup>21</sup> and in the synthetic schemes only novel compounds are numbered.

**Scheme 1<sup>a</sup>** Preparation of aldehyde building blocks for reductive amination as the last step

<sup>a</sup>Reagents and conditions: (i) NaCN, 3-hydroxyazetidinium chloride, TEA, MeOH, rt (55%); (ii) TEA, MsCl or TsCl, DCM, 0°C → rt (quant.); (iii) Cs<sub>2</sub>CO<sub>3</sub>, DMA, 110°C (48-81%).

**Scheme 2<sup>a</sup>** Synthesis of analogues **6**, **7**, **10** and **11** using ether formation as the last step

<sup>a</sup>Reagents and conditions: (i) Na(CH<sub>3</sub>CO<sub>2</sub>)<sub>3</sub>BH, TEA, DCM, rt (43%-quant); (ii) Cs<sub>2</sub>CO<sub>3</sub>, DMF or DMA, 90°C (6-51%).

1  
2  
3 Synthesis and medicinal chemistry of all compounds from the pyrimidine series (Table 4) have  
4  
5 been described earlier.<sup>27-29</sup>  
6

7  
8 To properly assess the extent of mEH-mediated metabolism, it was crucial to discriminate  
9  
10 between oxido-reductive and mEH-mediated hydrolytic ring-opening of the spiro-oxetane. Both  
11  
12 these metabolic steps can lead to the formation of hydrated (+18.0106 Da, *i.e.* +H<sub>2</sub>O) metabolites  
13  
14 (a mechanism for CYP-mediated oxetane hydration is proposed below). Experiments were  
15  
16 carried out in human liver microsomes (HLM) in the presence or absence of NADPH, a cofactor  
17  
18 for CYP enzymes but not for EH.<sup>23</sup>  
19  
20

21  
22 First, a set of analogues containing the spiro-oxetanylazetidiny building block with different  
23  
24 substitution patterns were investigated (entries **1-11**, Table 1). These compounds formed two  
25  
26 distinct hydrated (+18 Da) metabolites from either oxido-reductive ring-opening of the azetidine  
27  
28 or *via* hydrolytic and/or oxido-reductive ring opening of the oxetane. Structures of both +18 Da  
29  
30 metabolites were confirmed by UPLC-MS analysis of HLM incubations of the analogue **1**  
31  
32 alongside synthetic standards of both hydrolyzed oxetane (**12**) and ring-opened azetidine (**13**)  
33  
34 metabolites (See Supporting Information, Figure S1). For all compounds in this set (**1-11**),  
35  
36 formation of diol could be detected in the presence of NADPH and could account for as much as  
37  
38 15% of the total parent-related material (*cf* **1** and **6**; Table 1). In the absence of NADPH, diol  
39  
40 formation could be also detected for compounds **1-11**, suggesting mEH-mediated diol formation  
41  
42 (Table 1). For the majority of compounds in the spiro-oxetanylazetidiny series (Table 1), an  
43  
44 increase in diol formation was observed in the absence of NADPH, likely reflecting the higher  
45  
46 substrate availability to mEH-mediated hydrolysis in absence of a functional CYP system.  
47  
48 However, it is clear that subtle structural changes have a large impact on the metabolic fate of  
49  
50 compounds from this chemical series. For instance, *meta*-chloro substitution of the western  
51  
52  
53  
54  
55  
56  
57  
58  
59  
60

1  
2  
3 phenyl ring (entry **7**) followed the pattern observed for most compounds in the series, with an  
4  
5 increase of diol formation in the absence of NADPH. In contrast, *ortho*-chloro substitution of the  
6  
7 western phenyl ring (entry **6**) led to a higher proportion of diol formation in the presence of  
8  
9 NADPH. Diol formation could also be detected in the absence of NADPH for **6** but CYP-  
10  
11 mediated oxetane ring-opening to diol is the major pathway for this compound, similar to what  
12  
13 has previously been reported for other oxetane-containing compounds.<sup>14,30</sup> A possible reaction  
14  
15 mechanism for oxetane ring-opening to diol by CYP-mediated oxidation, proceeds *via*  $\alpha$ -  
16  
17 hydroxylation, spontaneous ring-opening to the aldehyde and finally reduction to diol by  
18  
19 aldehyde reductase.<sup>14,30</sup> The eastern phenyl chloro-substituted pair **6** and **7** exhibit similar  
20  
21 physicochemical properties, with slightly higher logD (3.0 and 2.7, respectively) and lower pK<sub>a</sub>  
22  
23 (7.5 and 7.7, respectively), as compared to the non-chlorinated analogue **2** (logD 1.8, pK<sub>a</sub> 8.0).  
24  
25 The western phenyl methyl-substituted matched pair **8** and **9** both show an increase of diol  
26  
27 formation in the absence of NADPH. For **8**, the diol metabolite increased fourfold in the absence  
28  
29 of NADPH (22% vs 5.2%, Table 1) and for **9**, a two-fold increase was observed. This pair can be  
30  
31 compared to **1**, which in addition, is also 4-methoxy-substituted in the eastern phenyl ring and  
32  
33 for which a decrease in diol formation was observed without NADPH. The introduction of a  
34  
35 methyl group in the western phenyl ring of **1** to yield **8** and **9** gave an increase in lipophilicity of  
36  
37 around 0.5 log units, an increase in overall hepatic metabolism and a higher proportion of non-  
38  
39 NADPH mediated diol formation.  
40  
41  
42  
43  
44  
45  
46  
47  
48  
49  
50  
51  
52  
53  
54  
55  
56  
57  
58  
59  
60

**Table 1.** Physicochemical parameters, metabolic clearance and fraction of diol metabolites formed in HLM from 2-oxa-6-azaspiro[3.3]heptanes (**1-11**).

Compound	Structure	Solubility ( $\mu\text{M}$ ) <sup>a</sup>	LogD <sup>a,b</sup>	pK <sub>a</sub> <sup>a</sup>	Hhep <sup>c</sup> CL <sub>int</sub> ( $\mu\text{l}/\text{min}/10^6$ cells)	% Diol in HLM w NADPH <sup>d</sup>	% Diol in HLM w/o NADPH <sup>d</sup>	% Amino alcohol w NADPH
1		91	2.0	8.2	10.5	15.6±0.3	5.9±0.1	0.7
2		89	1.8	8.0	6.1	1.7±0.1	2.7±0.3	<1
3		86	2.4	8.5	5.3	7.3±0.1	16±1	3.0±1.4
4		51	2.5	NA	27.2	<1%	4.2±0.1	2.4±0.6
5		735	2.0	8.2	1.9	1.2±0.0	3.5±0.2	1.9±0.5
6		90	3.0	7.7	32.7	15±0	6.3±0.4	1.7±1.7
7		76	2.7	7.5	12.4	2.9±2.9	8.6±0.2	0
8		73	2.6	8.2	17.0	5.2±1.1	22±1	<1
9		74	2.5	8.4	18.6	10±0	19±1	3.1±0.2
10		87	2.1	8.2	19.4	6.2±0.7	17±1	5.1±0.3
11		82	2.2	8.9	19.5	2.1±0.6	3.2±0.0	2.7±0.9

<sup>a</sup>Solubility, logD, pK<sub>a</sub> and CL<sub>int</sub> were measured as described previously<sup>31</sup>; <sup>b</sup>LogD<sub>7.4</sub> HPLC;

<sup>c</sup>Hhep, human hepatocytes; <sup>d</sup>HLM, human liver microsomes; average diol levels ± range were determined from duplicate incubations (60 min) of 10  $\mu\text{M}$  substrate either with HLM or without NADPH. Diol metabolite levels are expressed as a percentage of the sum of the total parent-related peak areas. All data are from reactions in absence of inhibitors.

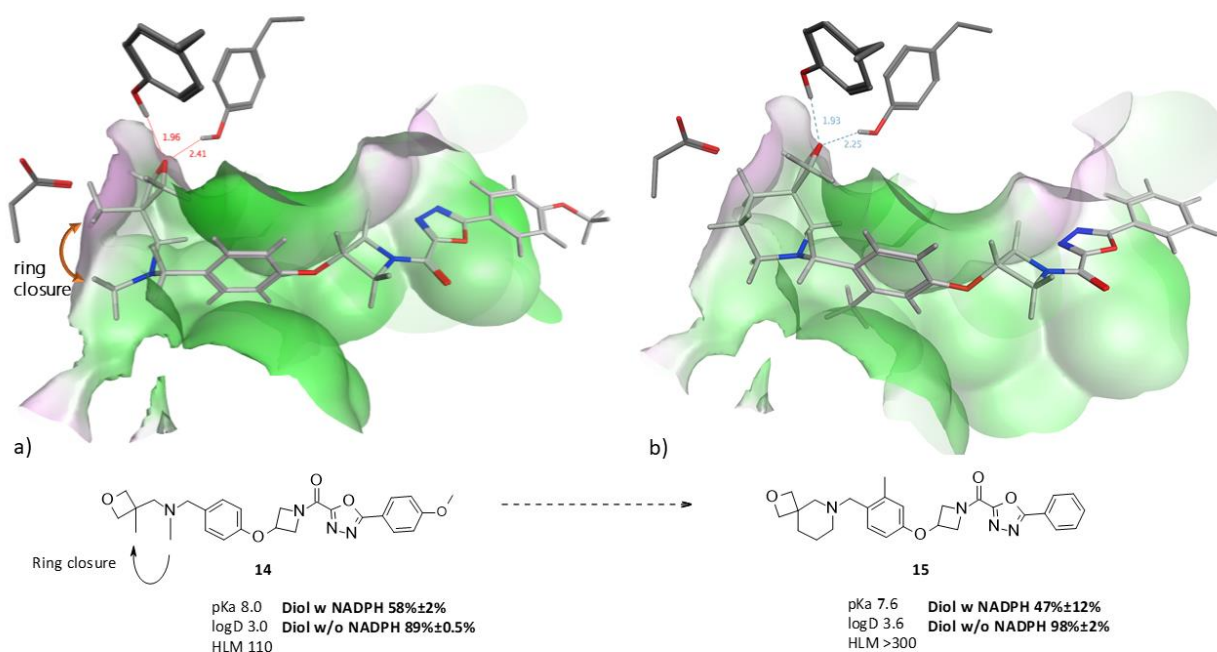
1  
2  
3 For the **1**, **8** and **9** trio, the correlation to logD can be made, but comparing **1-5**, all unsubstituted  
4 in the western phenyl region and with different 4-substituents of the eastern phenyl region, there  
5 is no clear correlation to lipophilicity and hepatic stability. For example, the most lipophilic  
6 compound of these (**4**, logD 2.5), which as expected shows the highest hepatic turnover, is  
7 metabolized to diol to a higher extent without NADPH. This is the case for all the examined  
8 unsubstituted western phenyl analogues, with the exception of **1**. This compound and the *ortho*-  
9 chloro substituted western phenyl **6** are the only analogues of those examined to show a higher  
10 degree of diol formation in the presence of NADPH.  
11  
12  
13  
14  
15  
16  
17  
18  
19  
20  
21

22 In conclusion, for the spiro-oxetanylazetidiny series there is no clear correlation between the  
23 measured physicochemical properties, logD and pK<sub>a</sub>, and mEH-mediated diol formation. Neither  
24 does a higher metabolic turnover in complementary studies using human hepatocytes (Table 1)  
25 correlate with a higher fraction of diol formed. However, it should be pointed out that the logD  
26 range in the series is not very wide. The difference in the degree of mEH-mediated metabolism is  
27 on the other hand quite significant, suggesting that introduction of an oxetane moiety can greatly  
28 affect metabolic clearance pathways even within a rather narrow physicochemical property  
29 space.  
30  
31  
32  
33  
34  
35  
36  
37  
38  
39  
40  
41

42 In an effort to better understand the observed SAR, we constructed a protein structure model of  
43 human mEH and performed docking studies of the substrates to the model structure. The human  
44 mEH model was constructed by comparative homology modelling using the crystal structure of  
45 juvenile hormone epoxide hydrolase from the silkworm *Bombyx mori* (PDB ID: 4QLA)<sup>32</sup> as  
46 template and using the aligned inhibitor valpromide from the crystal complex with the  
47 *Aspergillus niger* EH (PDB ID: 3G0I) in the model construction.<sup>33</sup> Compared to earlier published  
48 models,<sup>34,35</sup> the structure model presented here is based on templates with a significantly higher  
49  
50  
51  
52  
53  
54  
55  
56  
57  
58  
59  
60

1  
2  
3 degree of sequence identity overall and particularly so in the active site (see Figures S2 and S3  
4  
5 for more details of the homology model).

6  
7  
8 Initially, the *N*-methylated 3-methyloxetane analogue **14**<sup>25</sup> was used to guide docking and energy  
9  
10 minimizations in the active site (Figure 2a). Analysis of the low-energy binding mode of **14**  
11  
12 suggested that ring closure to a 3-oxetane piperidine spirocycle should constitute an excellent fit  
13  
14 in the active site, presenting the oxetane oxygen in an optimal orientation for catalysis (Figure  
15  
16 2b). A methyl-substituted analogue of the spiro-piperidine was available in the AstraZeneca  
17  
18 compound collection, **15**. When docking **15**, the western methyl substituent could adopt two  
19  
20 rotamers that both fitted into the enzyme binding site. The rotamer where the methyl is pointing  
21  
22 inwards has a slightly more optimal orientation of the oxetane moiety in the catalytic site. This  
23  
24 rotamer is shown in Figure 2b. The spiro-piperidine **15** indeed showed almost complete  
25  
26 conversion to diol in the absence of NADPH (Figure 2b).  
27  
28  
29  
30



1  
2  
3 **Figure 2.** Docking poses in the active site of the mEH protein structure model. The accessible  
4 surface of the protein, represented by how close an oxygen atom in a water molecule could be  
5 without any steric repulsion, is shown for the parts of the protein that are in close proximity to  
6 the ligand. Green color: hydrophobic areas, and purple: hydrophilic areas. The two tyrosines in  
7 the active site coordinating with the ring oxygen in the ligand (Y299 & Y374, O...H distances in  
8 Å) and the catalytic aspartic acid (D226) are shown. a) A docked pose and the 2D representation  
9 of **14**; b) A docked pose and the 2D representation of **15**. Data for the observed mEH-catalyzed  
10 oxetane hydrolysis of **14** and **15** is shown beneath each structure.

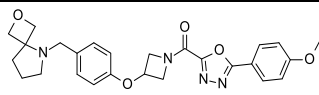
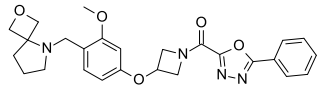
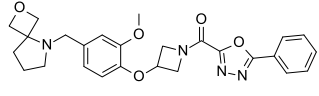
11  
12  
13  
14  
15  
16  
17  
18  
19  
20  
21  
22  
23 In contrast, the spiro compound **2** (Table 1), which shows lower degree of diol formation,  
24 cannot bind in a pose optimal for catalysis without minor steric clashes in the vicinity to the  
25 oxetane (Figure S4). The docking pose for **2** suggests a steric clash, with the oxygen atom of the  
26 oxetane penetrating through the interaction surface, shortened hydrogen bond distances and a  
27 slightly bent oxetane ring. This steric hindrance for compound **2** compared to the corresponding  
28 spiro-oxetane piperidine **15** suggests a marked difference in substrate turnover.

29  
30  
31  
32  
33  
34  
35  
36 Attempts to crystallize the mEH protein have been unsuccessful to date.<sup>36</sup> In the absence of X-  
37 ray data, we applied the homology model and guided dockings to the bicyclic oxetane series. For  
38 this series, the structural insights have been useful for understanding where the ligand vs active  
39 site shape and electrostatic complementarity set limits for the ligand to bind in a pose that is  
40 optimal for hydrolysis. The model was used to increase our qualitative understanding of mEH-  
41 mediated oxetane hydrolysis for the bicyclic oxetane series.

42  
43  
44  
45  
46  
47  
48  
49  
50 We then wanted to expand the investigation of mEH-catalyzed hydrolysis to other ring  
51 systems. The metabolism of a set of 2-spiro-oxetane pyrrolidines were investigated under the  
52 same conditions as before (Table 2, compounds **16-20**). NADPH-independent ring-opening of  
53  
54  
55  
56  
57  
58  
59  
60

the oxetane was again observed, but for these compounds diol formation was generally higher in the presence of NADPH, suggesting CYP-mediated oxidative diol formation is a more pronounced competing pathway for these substrates. It should be noted that these pyrrolidines are more lipophilic than the azetidines. However, this does not account for the increase in CYP-mediated oxetane ring openings observed *per se*. As shown, more lipophilic substrates, *e.g.* spiro piperidine **15**, are completely turned over by mEH (Figure 2). For the spiro pyrrolidines, western *ortho*-methoxy phenyl substitution attenuates CYP-independent diol formation. For **17**, no diol was formed in the absence of NADPH, suggesting that this compound is not a substrate of mEH. The analogue **19** was turned over by mEH, which is somewhat surprising as the eastern phenyl group according to our homology model would be partly outside the enzyme and substitutions of this region should have a minor impact on the turnover.

**Table 2.** Physicochemical parameters, metabolic clearance and fraction of diol metabolites formed in HLM from spiro oxetanes and tetrahydrofurans (**16-22**) and an embedded oxetane (**23**).

Compound	Structure	Solubility ( $\mu\text{M}$ ) <sup>a</sup>	LogD <sup>a,b</sup>	pKa <sup>a</sup>	Hhep <sup>c</sup> CL <sub>int</sub> ( $\mu\text{l}/\text{min}/10^6$ cells)	% Diol in HLM w NADPH <sup>d</sup>	% Diol in HLM w/o NADPH <sup>d</sup>	% Amino alcohol w NADPH
<b>16</b>		3	3.9	6.0	48.7	12±1	4.5±0.2	0
<b>17</b>		60	3.8	8.0	27.5	22±2	<1	0
<b>18</b>		221	3.5	6.0	25.0	23±2	15±3	0

19		43	4.2	7.0	42.7	5.1±0.4	2.9±0.1	0
20		39	3.8	6.1	38.5	22±1	28±0	0
21		82	2.2	8.6	10.8	0	<1	<1
22		495	2.7	ND	10.4	0	<1	<1
23		3	2.9	7.3	38.0	4.4±0.4	21±1	2.7±0.2

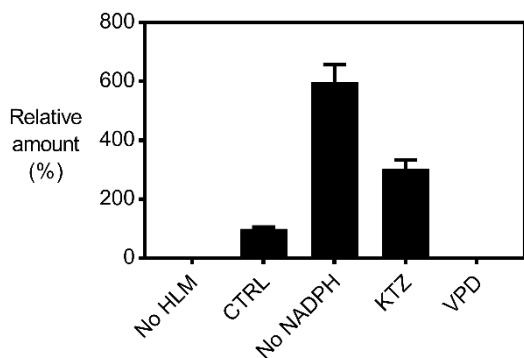
<sup>a</sup>Solubility, logD, pK<sub>a</sub> and CL<sub>int</sub> were measured as described previously<sup>31</sup>; <sup>b</sup>LogD<sub>7.4</sub> HPLC; <sup>c</sup>Hhep, human hepatocytes; <sup>d</sup>HLM, human liver microsomes; average diol levels ± range were determined from duplicate incubations (60 min) of 10 μM substrate either with HLM or without NADPH. Diol metabolite levels are expressed as a percentage of the sum of the total parent-related peak areas. All data are from reactions in absence of inhibitors.

The *meta*-methoxy substituted western phenyl spiro-pyrrolidines **18** and **20** were hydrolyzed by mEH to a much greater extent and for **20** even an increase in diol could be observed. Again, this finding was unexpected and warrants further study of the SAR of CYP- vs mEH-mediated oxetane ring-cleavage.

For spiro-tetrahydrofuran azetidines (Table 2, **21** and **22**), no diol formation of the less strained THF ring was detected in the absence of NADPH. The tetrahydrofuran ring of these compounds was also stable to oxidative ring opening. Nor did an extended set of compounds containing only tetrahydrofurans or tetrahydropyrans form any metabolites corresponding to the addition of water (data not shown). However, the bridged and rather strained oxetanyl piperidine ring (Table 2, **23**) was hydrolyzed to diol in the absence of NADPH. The observed increase in diol formation

1  
2  
3 was quite pronounced, demonstrating that mEH-catalyzed ring opening of oxetanes is not only  
4  
5 confined to spirocyclic ring systems or simple oxetanes.  
6

7  
8 These data suggested that bicyclic oxetane rings were opened *via* hydrolysis and that this  
9  
10 metabolic route may be enhanced in the absence of NADPH, i.e. in the absence of a functional  
11  
12 CYP system. We further investigated whether spiro-oxetane metabolism by mEH would increase  
13  
14 also in the presence of a potent CYP inhibitor. A subset of compounds was selected to  
15  
16 investigate this hypothesis: the 3-oxetane azetidines **3**, **4** and **5**, the 3-oxetane piperidine **15**, the  
17  
18 2-oxetane pyrrolidine **20**, the 3-tetrahydrofuran azetidine **21** and the bridged oxetane **23**. With  
19  
20 the exception of **21**, which was included as a negative control, the selected compounds all had  
21  
22 shown an increase in diol formation in the absence of NADPH (Tables 1 and 2). The compounds  
23  
24 were incubated with HLM in the presence of a high concentration of the potent CYP inhibitor  
25  
26 ketoconazole and NADPH. The observed diol formation pattern matched our previous  
27  
28 observations in the +/- NADPH experiments. Compounds **3**, **4**, **5**, **15**, **20** and **23** showed an  
29  
30 increase in diol formation in the presence of ketoconazole (see Figure 3 for a representative plot  
31  
32 for **23**), whereas this, as expected, was not the case for the 3-tetrahydrofuran-azetidine **21** (data  
33  
34 not shown). As seen in incubations devoid of NADPH (Figure 3 and Tables 1-2), an increase in  
35  
36 diol formation likely results from higher availability of the substrate to enzymes other than  
37  
38 CYPs, when these are inhibited by ketoconazole. To confirm the involvement of mEH, the same  
39  
40 set of compounds was also incubated with a high concentration of the selective mEH inhibitor  
41  
42 valpromide, this time abolishing diol formation (see Figure 3, for a representative plot for **23**).  
43  
44  
45  
46  
47  
48  
49  
50  
51  
52  
53  
54  
55  
56  
57  
58  
59  
60

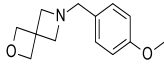
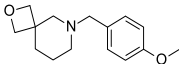
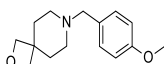
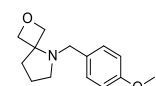


**Figure 3.** Hydration of **23** in selective conditions. No HLM, incubations without human liver microsomes; CTRL, incubations without inhibitors ([NADPH], 1 mM); No NADPH, incubations in absence of NADPH; KTZ, incubations in presence of the CYP inhibitor ketoconazole (200  $\mu$ M; [NADPH], 1 mM); VPD, incubations in presence of the mEH inhibitor valpromide (1 mM; [NADPH], 1 mM). Results are expressed as a % of CTRL reactions; bars are averages of duplicate measurements + range.

These results suggest that introduction of an oxetane can direct metabolism away from CYP enzymes, which can have an impact on the risk of DDI in a chemical series. Of course, this will vary considerably between different chemical lead series and, as we have shown, between similar compounds from the same series. Nonetheless, introduction of an oxetane in a lead series can be a way to avoid a high degree of metabolism by CYP enzymes.

In an effort to understand the minimum structural requirements for mEH-catalyzed hydrolysis, we prepared a representative set of truncated spirocyclic analogues and analyzed their biotransformation as described earlier (compounds **24-27**, Table 3).

**Table 3.** Physicochemical parameters, metabolic clearance and fraction of diol metabolites formed in HLM from truncated spiro-oxetanes

Compound	Structure	Solubility ( $\mu\text{M}$ ) <sup>a</sup>	LogD <sup>b</sup>	pK <sub>a</sub>	HLM <sup>c</sup> CL <sub>int</sub> ( $\mu\text{l}/\text{min}/\text{mg}$ )	% Diol in HLM w NADPH <sup>d</sup>	% Diol in HLM w/o NADPH <sup>d</sup>
<b>24</b>		364	0.40	8.25	<3	0	0
<b>25</b>		744	1.50	8.08	28.3	8.3±0.4	10.9±0.2
<b>26</b>		750	0.80	8.56	20.6	<1	1±0
<b>27</b>		610	1.80	ND	8.10	9.2±0.6	0

<sup>a</sup>Solubility, logD, pK<sub>a</sub> and CL<sub>int</sub> were measured as described earlier<sup>31</sup>; <sup>b</sup>LogD<sub>7.4</sub> HPLC; <sup>c</sup>HLM, human liver microsomes; <sup>d</sup>Average diol levels ± range were determined from duplicate incubations (60 min) of 10  $\mu\text{M}$  substrate with HLM. Diol metabolite levels are expressed as a percentage of the sum of the total parent-related peak areas. All data are from reactions in absence of inhibitors.

The shortened 3-oxetanyl-azetidine **24** was metabolically stable to human liver microsomes, presumably due to low lipophilicity. Both oxetane piperidines **25** and **26** were hydrolyzed to a greater extent by mEH in the absence of NADPH, but the turnover increase of **25** is much less pronounced than for the “full-length” analogue **15**. For **27**, formation of the diol metabolite was NADPH-dependent and completely inhibited by ketoconazole, rather than valpromide (Figure 4a). This is consistent with a CYP-mediated oxidative biotransformation and matches the findings for the spiro-oxetanyl-pyrrolidines of the long-chain series, particularly **17**. To confirm that addition of water occurred on the oxetane and not on the pyrrolidine, an authentic oxetane ring-opened diol standard of **27** was synthesized (compound **28**). When the reaction mixture from incubations of **27** with HLM and NADPH was co-chromatographed with **28** they were found to co-elute by UPLC-MS, thus confirming the spiro-oxetane of this truncated compound was ring-opened *via* an oxidation/reduction sequence catalyzed by CYPs and a reductase (e.g.

1  
2  
3 aldehyde reductase) as mentioned previously<sup>30</sup>, forming the diol metabolite **28** (Figures 4b and  
4  
5  
6 4c).

7  
8 We were then interested to understand whether mEH-catalyzed oxetane hydrolysis was  
9  
10 significant in a structurally-unrelated chemical series. A search in the AstraZeneca compound  
11  
12 collection was made and a series of oxetane-substituted pyrimidines were selected.<sup>27-29</sup>  
13  
14 For the set of compounds selected (Table 4), matched pairs were available where the oxetane  
15  
16 moiety was attached to the pyrimidine core *via* either amine or ether linkers. Again, the overall  
17  
18 metabolism in HLM and diol formation in the presence and absence of NADPH was investigated  
19  
20 as described earlier. For the amine-linked pyrimidines **29**, **31** and **33**, oxetane ring-opening  
21  
22 increased in the absence of NADPH (Table 4). Additional experiments showed that oxetane  
23  
24 cleavage was completely inhibited by valpromide, was unaffected by ketoconazole and was  
25  
26 NADPH-independent in HLM (see Figure 4d for a representative plot for **29**). Similar results  
27  
28 were obtained in human hepatocytes (data not shown). Hydrolysis was also unaffected by the  
29  
30 soluble EH (sEH) inhibitor *t*-AUCB and was absent in human liver cytosol (HLC), ruling out the  
31  
32 contribution of sEH (data not shown). Interestingly, the oxetane ether-linked pyrimidine matched  
33  
34 pairs **30**, **32** and **34** were completely stable to oxetane hydrolysis (Table 4).  
35  
36  
37  
38  
39  
40  
41  
42  
43  
44  
45  
46  
47  
48  
49  
50  
51  
52  
53  
54  
55  
56  
57  
58  
59  
60

**Table 4.** Physicochemical parameters, metabolic clearance and fraction of diol metabolites formed in HLM from N- and O-linked oxetane substituted pyrimidines (**29-34**) and N and O-linked methyl oxetanes **35** and **36**.

Compound	Structure	Solubility ( $\mu\text{M}$ ) <sup>a</sup>	LogD <sup>b</sup>	pK <sub>a</sub>	HLM <sup>c</sup> CL <sub>int</sub> ( $\mu\text{l}/\text{min}/\text{mg}$ )	% Diol in HLM w NADPH <sup>d</sup>	% Diol in HLM w/o NADPH <sup>d</sup>
<b>29</b>		580	1.1	2.8	<2	21±0	27±0
<b>30</b>		867	2.0	ND	<2	0	0
<b>31</b>		>2520	1.6	2.4	<3.5	8.5±0.2	12±0
<b>32</b>		818	1.6	ND	6.1	0	0
<b>33</b>		>1820	2.1	2.6	<2	9.4±0.6	14±0
<b>34</b>		476	1.9	2.6	2.8	0	0
<b>35</b>		61	2	8.2	103	32±0	31±0
<b>36</b>		3	ND	ND	>300	79±21	98±3

<sup>a</sup>Solubility, logD, pK<sub>a</sub> and CL<sub>int</sub> were measured as described earlier<sup>31</sup>; <sup>b</sup>LogD<sub>7.4</sub> HPLC; <sup>c</sup>HLM, human liver microsomes; <sup>d</sup>Average diol levels ± range were determined from duplicate incubations (60 min) of 10  $\mu\text{M}$  substrate with HLM. Diol metabolite levels are expressed as a percentage of the sum of the total parent-related peak areas. All data are from reactions in absence of inhibitors. ND, not determined.

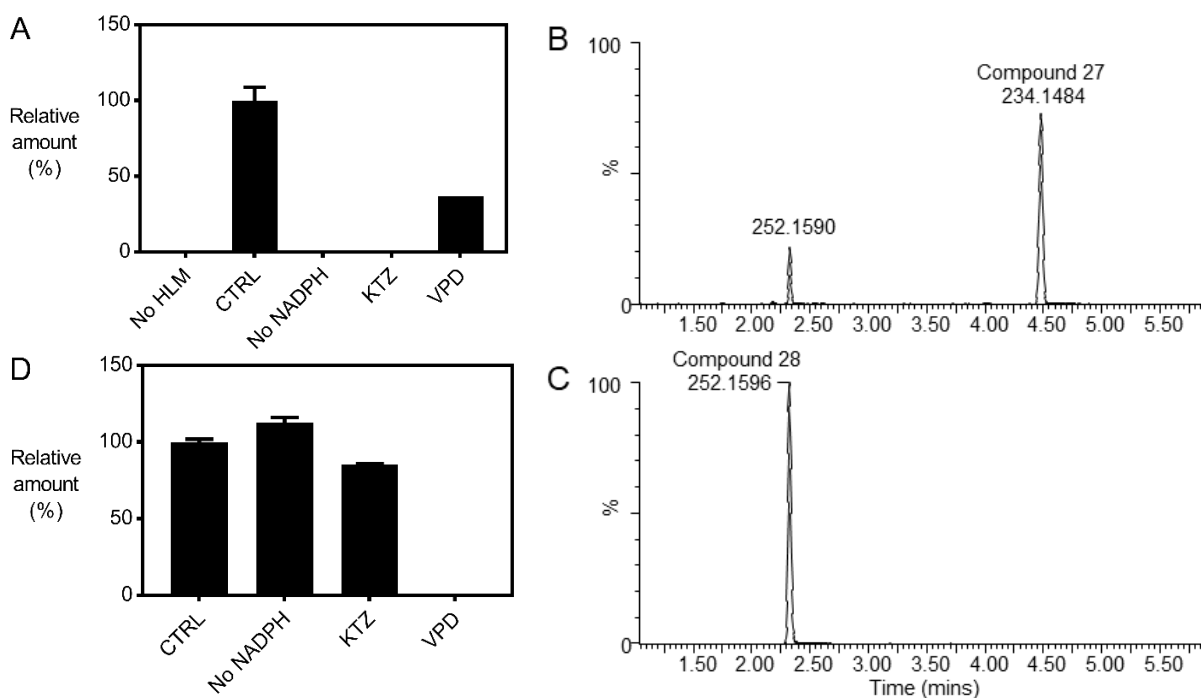


**Figure 4.** A) Hydrolysis of **27**; B) and C) UPLC-MS extracted ion chromatograms for: compound **27** and its hydrated metabolite formed in an incubation with HLMs and NADPH (B); synthetic diol **28** (C). Peak labels are  $m/z$  values and correspond to parent ( $m/z$  234.1484) and hydrated metabolite ( $m/z$  252.1596). D) Hydrolysis of **29**. Abbreviations in panels A and D are as defined in the legend for Figure 3. Results are expressed as a % of CTRL reactions; bars are averages of duplicate measurements + range.

The matched pair **29** and **30** could both be docked into the active site of the homology model in a pose suitable for catalysis, as shown in Figure 5. Hence, the lack of diol formation of **30** in the absence of NADPH could not be explained by how it fits into the active site of the model. The proximity of the amine/ether link to the site of hydrolysis suggests that this may be due to a reactivity difference between the anilinic and phenolic oxetane substituent in **29** and **30**,

1  
2  
3 respectively. Furthermore, dockings with the amine-linked pyrimidines **29**, **31** and **33** (Figure  
4  
5 S5) revealed a trend towards more steric hindrance with increasing size of cyclic alkyls resulting  
6  
7 in a docking pose for the cyclopentyl-substituted pyrimidine **33** clearly less optimal for catalysis.  
8  
9 However, the difference in diol formation in absence of NADPH between the cyclopropyl-  
10  
11 substituted pyrimidine **29** and the cyclobutyl-substituted pyrimidine **31** could not be resolved by  
12  
13 the model.  
14  
15

16  
17 This prompted us to incorporate an ether linker between the proximal phenyl ring and the  
18  
19 terminal methyl oxetane. For this purpose, compound **36** was synthesized to form a matched pair  
20  
21 with the simple oxetane **35** and subjected to the same battery of assays (Table 4).  
22  
23

24 To our surprise, the opposite relationship was observed, with oxetane hydrolysis in the absence  
25  
26 of NADPH increasing from 31% with the amine-linked compound **35** to 98% with the ether  
27  
28 linked **36** (Table 4). In an attempt to rationalize this finding, the homology model was revisited.  
29  
30 A closer look at the binding site suggested that the substrates with spirocyclic amines or their  
31  
32 corresponding ring-opened analogues would bind more strongly in their neutral states.  
33  
34

35 This can be deduced from the lipophilic nature of the binding site region. Introduction of a  
36  
37 positive charge in this lipophilic cavity would decrease affinity for the ligand and reduce diol  
38  
39 formation. This may be an explanation as to why the ether analogue **36** shows such a high degree  
40  
41 of diol formation, as it is neutral. However, it should be pointed out that there is no general trend  
42  
43 towards higher degree of diol formation for amine substrates with a lower  $pK_a$  within the  $pK_a$   
44  
45 range examined. Again, this is an example of how structural changes in other regions of the  
46  
47 molecule aside from the oxetane ring system can have a marked effect on the metabolic fate and  
48  
49 these effects appear to vary between chemical series.  
50  
51  
52  
53  
54  
55  
56  
57  
58  
59  
60

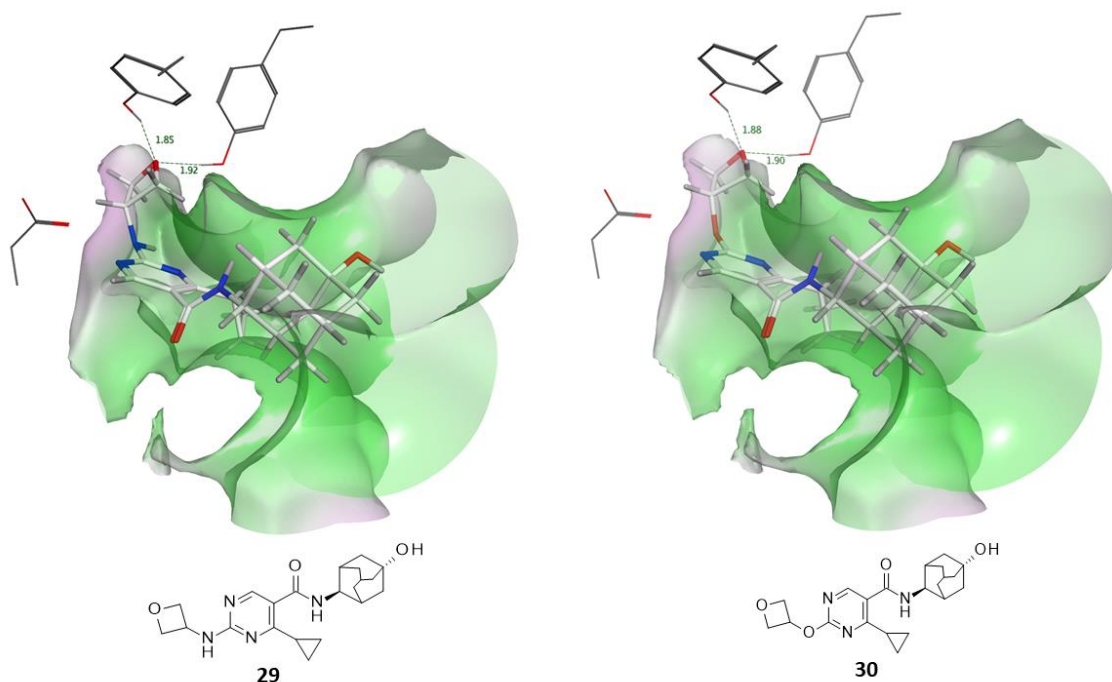


**Figure 5.** Docking poses of **29** (left) and **30** (right) in the active site of the mEH protein structure model. The accessible surface of the protein, represented by how close an oxygen atom in a water molecule could be without any steric repulsion, is shown for the parts of the protein that are in close proximity to the ligand. Green color: hydrophobic areas and purple: hydrophilic areas. The two tyrosines in the active site coordinating with the ring oxygen in the ligand (Y299 & Y374, O...H distances in Å) and the catalytic aspartic acid (D226) are shown.

A set of electronic properties were also calculated using both semi-empirical QM (am1 and pm3) and density functional theory B3LYP/6-31G\* calculations.<sup>37</sup> Both LUMO energies and partial charges for the oxygen and surrounding carbon atoms in the oxetane/tetrahydrofuran rings were calculated using the methods described above. Calculations were performed for the oxetane/tetrahydrofuran containing fragments which included substitutions that affect reactivity (11 fragments in total were identified in the dataset). LUMO energy calculations using semi-

1  
2  
3 empirical methods were also performed on intact molecules. No correlations between these  
4  
5 electronic properties and the degree of diol formation w/o NADPH were found in the dataset  
6  
7 (data not shown). The most likely explanation for this lack of correlation is that the degree of  
8  
9 hydrolytic ring-opening is related to both the fit of the substrate to the active site and the  
10  
11 reactivity of the substrate. These factors would not necessarily be individually correlated with the  
12  
13 calculated physicochemical properties and the combination most certainly not.  
14  
15  
16  
17  
18

## 19 CONCLUSIONS

20  
21 Building on our previous work<sup>22,25</sup> we have considerably expanded our knowledge on the  
22  
23 chemical space of non-epoxide substrates of mEH. Our findings demonstrate that short- and  
24  
25 long-chain bicyclic oxetanes as well as a second structurally distinct compound series containing  
26  
27 simple oxetanes are turned over by mEH, confirming that hydrolysis by mEH is not confined to  
28  
29 oxiranyl substrates only.  
30  
31  
32

33 A homology model of human mEH was developed, that is improved with respect to sequence  
34  
35 similarity as compared to earlier models described in the literature.<sup>34,35</sup> The structural insights  
36  
37 from the homology model and guided dockings were useful for understanding the limits for the  
38  
39 ligand to bind in a pose which was optimal for hydrolysis by mEH. With this model we can  
40  
41 partially understand and explain the SAR in terms of degree of diol formation.  
42  
43  
44

45 There were no clear correlations between the degree of oxetane hydrolysis and  
46  
47 physicochemical properties such as  $pK_a$  and logD or from calculated electronic properties i.e.  
48  
49 LUMO energies or partial charges.<sup>37</sup> This study shows that hydrolytic ring-opening is an  
50  
51 important metabolic pathway for oxetanes over different ring systems and that substitution and  
52  
53 small structural changes within a chemical series can greatly affect non-oxidative pathways. This  
54  
55  
56  
57  
58  
59  
60

1  
2  
3 study also demonstrates that it is possible to direct a compound's metabolic clearance *via* mEH  
4  
5 by careful selection of substituted bicyclic or simple oxetanes. Thus, by decreasing the  
6  
7 dependence on CYP-mediated oxidations, metabolic stability may be optimized and drug-drug  
8  
9 interaction risk decreased.

10  
11  
12 Attempts at modulating the clearance of small molecules to non-CYP mediated pathways is  
13  
14 however not without risk. Human PK may be poorly predicted, since knowledge around mEH  
15  
16 biology is relatively limited compared to the CYP system. Problems have been observed with  
17  
18 AO-driven clearance recently and have led to clinical failure,<sup>5-8</sup> though improvements to AO  
19  
20 scaling using *e.g.* multispecies allometry have recently been reported.<sup>38</sup> mEH is known to be  
21  
22 widely expressed in human tissues, where it may also take part in physiological function, and  
23  
24 polymorphic variants have been reported<sup>23, 24, 39, 40</sup> indicating possible risks for exposure  
25  
26 underprediction and inter-individual variability for the metabolism of its substrates.  
27  
28  
29

30  
31 Further fundamental research into this important non-CYP drug-metabolizing enzyme is thus  
32  
33 warranted and we strongly recommend that screening for mEH-mediated metabolism is included  
34  
35 in drug discovery projects with oxetane-containing lead series.  
36  
37  
38  
39

## 40 EXPERIMENTAL SECTION

41  
42 **General Chemistry.** Purchased chemicals were reagent-grade and used without purification.  
43  
44 <sup>1</sup>H NMR spectra were recorded at 400, 500 or 600 MHz Chemical shifts (ppm) and were  
45  
46 determined relative to internal solvent ( $\delta$  7.26 ppm; CDCl<sub>3</sub>,  $\delta$  2.50 ppm; DMSO-*d*<sub>6</sub>,  $\delta$  3.31 ppm;  
47  
48 MeOD). Microwave-assisted synthesis was carried out in an Initiator synthesizer single mode  
49  
50 cavity instrument producing controlled irradiation with a power range 0–400 W at 2450 MHz  
51  
52 (Biotage AB, Uppsala, Sweden). Analytical HPLC/MS was conducted on a QTOF mass  
53  
54  
55  
56  
57  
58  
59  
60

1  
2  
3 spectrometer using a UV detector monitoring either at (a) 210 nm with a BEH C18 column (2.1  
4 mm × 100 mm, 1.7 μm, 0.7 mL/min flow rate), using a gradient of 2% v/v ACN in H<sub>2</sub>O  
5  
6 (ammonium carbonate buffer, pH 10) to 98% v/v ACN in H<sub>2</sub>O, or at (b) 230 nm with an HSS  
7  
8 C18 column (2.1 mm × 100 mm, 1.8 μm, 0.7 mL/min flow rate), using a gradient of 2% v/v  
9  
10 ACN in H<sub>2</sub>O (ammonium formate buffer, pH 3) to 98% v/v ACN in H<sub>2</sub>O. Preparative HPLC was  
11  
12 performed by Waters Fraction Lynx with ZQ MS detector on either a Waters Xbridge C18 OBD  
13  
14 5 μm column (19×150 mm, flow rate 30 mL/min or 30×150 mm, flow rate 60 mL/min) using a  
15  
16 gradient of 5–95% ACN with 0.2% NH<sub>3</sub> at pH 10 or a Waters SunFire C18 OBD 5 μm column  
17  
18 (19×150 mm, flow rate 30 mL/min or 30×150 mm, flow rate 60 mL/min) using a gradient of 5–  
19  
20 95% ACN with 0.1 M formic acid. Automated flash chromatography was performed on a  
21  
22 Biotage system using a SiO<sub>2</sub> column and UV detection. High-resolution mass spectrometry  
23  
24 (HRMS) was carried out using high-resolution electrospray ionization mass spectrometry where  
25  
26 the spectrometer was linked together with an Acquity UPLC system. All tested compounds were  
27  
28 determined to be ≥95% pure using the analytical method a or b described above based on the  
29  
30 peak area percentage.  
31  
32  
33  
34  
35  
36  
37  
38  
39

40 Compounds **1**, **2**, **16**, **21** and **22** as well as intermediates 6-(4-(azetidin-3-yloxy)benzyl)-2-oxa-6-  
41  
42 azaspiro[3.3]heptane, 4-(1-(5-(4-methoxyphenyl)-1,3,4-oxadiazole-2-carbonyl)azetidin-3-  
43  
44 yloxy)benzaldehyde, 4-((1-(5-phenyl-1,3,4-oxadiazole-2-carbonyl)azetidin-3-  
45  
46 yl)oxy)benzaldehyde, 1-(5-(4-methoxyphenyl)-1,3,4-oxadiazole-2-carbonyl)azetidin-3-yl  
47  
48 methanesulfonate, 1-(5-phenyl-1,3,4-oxadiazole-2-carbonyl)azetidin-3-yl methanesulfonate and  
49  
50 (3-hydroxyazetidin-1-yl)(5-phenyl-1,3,4-oxadiazol-2-yl)methanone were all synthesized as  
51  
52 previously described.<sup>21</sup> All 5-phenyl-1,3,4-oxazole intermediates were synthesized from the  
53  
54  
55  
56  
57  
58  
59  
60

1  
2  
3 corresponding benzohydrazines.<sup>42</sup> Compounds **29**, **30**, **31**, **32**, **33** and **34** have previously been  
4 described.<sup>27</sup> Compounds **14** and **35** were synthesized according to a previously described  
5 procedure.<sup>25</sup>  
6  
7  
8  
9

10  
11 **(3-(4-(2-oxa-6-azaspiro[3.3]heptan-6-ylmethyl)phenoxy)azetidin-1-yl)(5-(4-**  
12 **(difluoromethyl)phenyl)-1,3,4-oxadiazol-2-yl)methanone (3).**

13  
14  
15 *(5-(4-(difluoromethyl)phenyl)-1,3,4-oxadiazol-2-yl)-(3-hydroxyazetidin-1-yl)methanone (37).*

16  
17 Ethyl 5-(4-(difluoromethyl)phenyl)-1,3,4-oxadiazole-2-carboxylate (1.0 g, 3.73 mmol) and  
18 azetidin-3-ol hydrochloride (490 mg, 4.47 mmol) were mixed in MeOH (20 mL). TEA (0.62 mL,  
19 4.47 mmol) was added followed by NaCN (0.18 g, 3.73 mmol) and the reaction was stirred at rt  
20 for 2 days. Most of the MeOH was evaporated off and water (20 mL) was added into the residue.  
21 The mixture was stirred for 5 min and the formed precipitate was filtered off, washed with water  
22 (10 mL) and dried under vacuum to afford **37** (603 mg, 55%). <sup>1</sup>H NMR (400 MHz, CDCl<sub>3</sub>) δ  
23 8.26 (d, *J* = 7.3 Hz, 2H), 7.69 (d, *J* = 7.3 Hz, 2H), 6.72 (t, *J* = 56 Hz, 1H), 4.75 – 5.11 (m, 2H),  
24 4.43 – 4.69 (m, 2H), 4.16 (d, *J* = 10.6 Hz, 1H), 2.39 (s, 1H).  
25  
26  
27  
28

29  
30  
31 *(1-(5-(4-(difluoromethyl)phenyl)-1,3,4-oxadiazole-2-carbonyl)azetidin-3-yl) methanesulfonate*

32  
33  
34 **(38).** **37** (603 mg, 2.04 mmol) was dissolved in DCM (10 mL) and cooled in an ice-bath. TEA  
35 (0.311 mL, 2.25 mmol) was added and then MsCl (0.167 mL, 2.14 mmol) was added dropwise  
36 over 5 min. The ice-bath was removed and the reaction stirred to rt for 3h. More DCM and aq.  
37 NaHCO<sub>3</sub> were added, the mixture filtered through a phase separator and evaporated to give **38**  
38 (807 mg, 106%). <sup>1</sup>H NMR (400 MHz, CDCl<sub>3</sub>) δ 8.26 (d, *J* = 8.2 Hz, 2H), 7.70 (d, *J* = 8.2 Hz,  
39 2H), 6.72 (t, *J* = 56 Hz, 1H), 5.34 – 5.48 (m, 1H), 5.06 – 5.20 (m, 1H), 4.83 – 4.95 (m, 1H), 4.59  
40 – 4.72 (m, 1H), 4.37 – 4.50 (m, 1H), 3.13 (s, 3H).  
41  
42  
43  
44  
45  
46  
47  
48  
49  
50  
51  
52  
53  
54  
55  
56  
57  
58  
59  
60

1  
2  
3 *4-(1-(5-(4-(difluoromethyl)phenyl)-1,3,4-oxadiazole-2-carbonyl)azetidin-3-yl)oxybenzaldehyde*  
4  
5 (**39**). **38** (800 mg, 2.14 mmol), 4-hydroxybenzaldehyde (275 mg, 2.25 mmol) and cesium  
6 carbonate (733 mg, 2.25 mmol) were mixed in DMA (10 mL) and stirred at 100°C over night.  
7  
8 After cooling to rt, EtOAc was added to the reaction mixture which was washed with water (4x),  
9  
10 dried (MgSO<sub>4</sub>) and evaporated. The residue was purified by automated flash chromatography on  
11  
12 a 50g column. A gradient from 30% to 100% of EtOAc in heptane over 15CV was used as  
13  
14 mobile phase. The product was collected using the wavelength 272 nm. Relevant fractions were  
15  
16 pooled and evaporated to afford **39** (333 mg, 39%). <sup>1</sup>H NMR (400 MHz, CDCl<sub>3</sub>) δ 9.93 (s, 1H),  
17  
18 8.27 (d, *J* = 8.4 Hz, 2H), 7.85 – 7.93 (m, 2H), 7.70 (d, *J* = 8.2 Hz, 2H), 6.91 (d, *J* = 8.7 Hz, 2H),  
19  
20 6.79 (t, *J* = 56 Hz, 1H), 5.14 – 5.25 (m, 2H), 4.77 – 4.86 (m, 1H), 4.72 (dd, *J* = 6.2, 12 Hz, 1H),  
21  
22 4.38 (dd, *J* = 2.1, 11.7 Hz, 1H).  
23  
24  
25  
26  
27

28 *(3-(4-(2-oxa-6-azaspiro[3.3]heptan-6-ylmethyl)phenoxy)azetidin-1-yl)(5-(4-*  
29  
30 *(difluoromethyl)phenyl)-1,3,4-oxadiazol-2-yl)methanone (3)*. **39** (55 mg, 0.14 mmol), 2-oxa-6-  
31  
32 azaspiro[3.3]heptane oxalate (32 mg, 0.17 mmol) and TEA (0.057 mL, 0.41 mmol) were mixed  
33  
34 in DCM (2 mL) and stirred at rt for 30 min. Sodium triacetoxyhydroborate (58 mg, 0.28 mmol)  
35  
36 was added and the reaction was stirred at rt over weekend. NaHCO<sub>3</sub> (sat. 2 mL) and DCM (2  
37  
38 mL) were added, the mixture stirred, filtered through a phase separator and evaporated. The  
39  
40 product was purified by preparative HPLC eluting with a gradient of ACN (5-95%) in 0.2%  
41  
42 ammonia buffer to afford **3** (40 mg, 60%). <sup>1</sup>H NMR (400 MHz, CDCl<sub>3</sub>) δ 8.26 (d, *J* = 8.3 Hz,  
43  
44 2H), 7.69 (d, *J* = 8.2 Hz, 2H), 7.19 (d, *J* = 8.6 Hz, 2H), 6.88 – 6.55 (m, 3H), 5.18 – 5.03 (m, 2H),  
45  
46 4.79 – 4.75 (m, 1H), 4.74 (s, 4H), 4.69 – 4.61 (m, 1H), 4.37 – 4.30 (m, 1H), 3.50 (s, 2H), 3.38 (s,  
47  
48 4H). HRMS calcd for C<sub>25</sub>H<sub>25</sub>F<sub>2</sub>N<sub>4</sub>O<sub>4</sub><sup>+</sup>, [M+H]<sup>+</sup>, 483.1844; found 483.1884.  
49  
50  
51  
52  
53  
54  
55  
56  
57  
58  
59  
60

1  
2  
3 **(3-(4-(2-oxa-6-azaspiro[3.3]heptan-6-ylmethyl)phenoxy)azetidin-1-yl)(5-(4-**  
4 **(difluoromethoxy)phenyl)-1,3,4-oxadiazol-2-yl)methanone (4).** Ethyl 5-(4-  
5  
6 (difluoromethoxy)phenyl)-1,3,4-oxadiazole-2-carboxylate (60 mg, 0.21 mmol) and 6-(4-  
7  
8 (azetidin-3-yloxy)benzyl)-2-oxa-6-azaspiro[3.3]heptane (50 mg, 0.19 mmol) were mixed in  
9  
10 MeOH (6 mL). NaCN (3.8 mg, 0.08 mmol) was added and the reaction was stirred at rt for 3 h.  
11  
12 The mixture was diluted with DCM (50 mL), the organic layer washed with Na<sub>2</sub>CO<sub>3</sub> (aq), dried  
13  
14 by filtering through a phase separator and evaporated. The crude product was purified by Si flash  
15  
16 column chromatography (first eluting with EtOAc (250 mL) and then eluting the product with  
17  
18 DCM : MeOH (2M NH<sub>3</sub>) 20:1) to afford **4** (65 mg, 68%). <sup>1</sup>H NMR (500 MHz, CDCl<sub>3</sub>) δ 8.18 (d,  
19  
20 *J* = 8.7 Hz, 2H), 7.35 – 7.18 (m, 4H), 6.84 – 6.44 (m, 3H), 5.17 – 5.04 (m, 2H), 4.76 (bs, 4H),  
21  
22 4.70 – 4.60 (m, 2H), 4.43 – 4.29 (m, 2H), 4.13 – 3.94 (m, 1H), 3.61 (bs, 4H). HRMS calcd for  
23  
24 C<sub>25</sub>H<sub>25</sub>F<sub>2</sub>N<sub>4</sub>O<sub>5</sub><sup>+</sup>, [M + H]<sup>+</sup>, 499.1793; found 499.1767.  
25  
26  
27  
28  
29  
30

31 **(3-(4-(2-oxa-6-azaspiro[3.3]heptan-6-ylmethyl)phenoxy)azetidin-1-yl)(5-(4-fluorophenyl)-**  
32 **1,3,4-oxadiazol-2-yl)methanone (5).** Ethyl 5-(4-fluorophenyl)-1,3,4-oxadiazole-2-carboxylate  
33  
34 (55 mg, 0.23 mmol) and 6-(4-(azetidin-3-yloxy)benzyl)-2-oxa-6-azaspiro[3.3]heptane (55 mg,  
35  
36 0.21 mmol) were mixed in MeOH (6 mL). NaCN (4.1 mg, 0.08 mmol) was added and the  
37  
38 reaction was stirred at rt for 3 h. The mixture was diluted with DCM (50 mL), washed with  
39  
40 Na<sub>2</sub>CO<sub>3</sub> (aq), dried by filtering through a phase separator and evaporated. The crude product was  
41  
42 purified by Si flash column chromatography (first eluting with EtOAc and then eluting the  
43  
44 product with DCM:MeOH (2M NH<sub>3</sub>) 20:1) to afford **5** (75 mg, 79%). <sup>1</sup>H NMR (500 MHz,  
45  
46 CDCl<sub>3</sub>) δ 8.23 – 8.12 (m, 2H), 7.31 – 7.11 (m, 4H), 6.73 (d, *J* = 8.5 Hz, 2H), 5.17 – 5.00 (m,  
47  
48 2H), 4.79 – 4.69 (m, 5H), 4.69 – 4.59 (m, 1H), 4.32 (dd, *J* = 11.5, 2.5 Hz, 1H), 3.49 (s, 2H), 3.37  
49  
50 (s, 4H). HRMS calcd for C<sub>24</sub>H<sub>24</sub>FN<sub>4</sub>O<sub>4</sub><sup>+</sup>, [M+H]<sup>+</sup>, 451.1781; found 451.1773.  
51  
52  
53  
54  
55  
56  
57  
58  
59  
60

1  
2  
3 **(3-(4-(2-oxa-6-azaspiro[3.3]heptan-6-ylmethyl)-3-chlorophenoxy)azetidin-1-yl)(5-phenyl-**  
4  
5 **1,3,4-oxadiazol-2-yl)methanone (6).**

6  
7 *3-chloro-4-(2-oxa-6-azaspiro[3.3]heptan-6-ylmethyl)phenol (40)*. 2-Chloro-4-hydroxy-  
8  
9 benzaldehyde (0.5 g, 3.19 mmol) and 2-oxa-6-azaspiro[3.3]heptane (0.55 g, 3.83 mmol) were  
10  
11 mixed in DCM (35 mL). After stirring for 20 min, sodium triacetoxyborohydride (1.02 g, 4.79  
12  
13 mmol) was added and the reaction mixture stirred at rt overnight. The mixture was diluted with  
14  
15 DCM and transferred to a separatory funnel. Water was added and the organic phase was rinsed  
16  
17 out (the product is in the water layer). The water phase was saturated with K<sub>2</sub>CO<sub>3</sub> and DCM was  
18  
19 added (organic phase is placed above the saturated water layer). The organic layers were  
20  
21 separated and the saturated water phase was extracted two more times with DCM. The organic  
22  
23 layers were combined, dried (phase separator) and concentrated to give **40** (0.653 g, 85%). <sup>1</sup>H  
24  
25 NMR (500 MHz, CDCl<sub>3</sub>) δ 7.09 (d, *J* = 8.4 Hz, 1H), 6.71 (d, *J* = 2.5 Hz, 1H), 6.55 (dd, *J* = 2.5,  
26  
27 8.4 Hz, 1H), 4.74 (s, 4H), 3.62 (s, 2H), 3.50 (s, 4H). LCMS (ES-) *m/z* [M - H]<sup>-</sup>: 238.1.

28  
29 *(3-(4-(2-oxa-6-azaspiro[3.3]heptan-6-ylmethyl)-3-chlorophenoxy)azetidin-1-yl)(5-phenyl-1,3,4-*  
30  
31 *oxadiazol-2-yl)methanone (6)*. **40** (0.33 g, 1.38 mmol) was dissolved in dry DMF (10 mL) and  
32  
33 Cs<sub>2</sub>CO<sub>3</sub> (0.90 g, 2.75 mmol) was added. The reaction mixture was stirred for 10 min before 1-(5-  
34  
35 phenyl-1,3,4-oxadiazole-2-carbonyl)azetidin-3-yl methanesulfonate (0.67 g, 2.07 mol) was  
36  
37 added. The reaction mixture was stirred at 90°C for 24 h, then filtered and evaporated. The  
38  
39 residue was purified by preparative HPLC eluting with a gradient of ACN (15-55%) in 0.2%  
40  
41 ammonia buffer to afford the product. <sup>1</sup>H-NMR revealed a minor impurity, so the product was  
42  
43 re-purified by silica gel chromatography eluting the product with DCM/MeOH(2M NH<sub>3</sub>) 20:1  
44  
45 followed by trituration with diethyl ether to afford **6** (213 mg, 33%). <sup>1</sup>H NMR (500 MHz,  
46  
47 CDCl<sub>3</sub>) δ 8.21 – 8.10 (m, 2H), 7.65 – 7.49 (m, 3H), 7.28 (d, *J* = 8.5 Hz, 1H), 6.79 (d, *J* = 2.5 Hz,  
48  
49  
50  
51  
52  
53  
54  
55  
56  
57  
58  
59  
60

1  
2  
3 1H), 6.68 (dd,  $J = 8.5, 2.5$  Hz, 1H), 5.17 – 5.10 (m, 1H), 5.08 – 5.01 (m, 1H), 4.79 – 4.71 (m,  
4 5H), 4.68 – 4.61 (m, 1H), 4.36 – 4.28 (m, 1H), 3.60 (s, 2H), 3.44 (s, 4H). HRMS calcd for  
5  
6  $C_{24}H_{24}ClN_4O_4^+$   $[M+H]^+$ , 467.1486; found 467.1495.  
7  
8  
9

10  
11 **(3-(4-(2-oxa-6-azaspiro[3.3]heptan-6-ylmethyl)-2-chlorophenoxy)azetidin-1-yl)(5-phenyl-**  
12  
13 **1,3,4-oxadiazol-2-yl)methanone (7).**  
14  
15

16 *2-chloro-4-(2-oxa-6-azaspiro[3.3]heptan-6-ylmethyl)phenol (41)*. 2-Oxa-6-azaspiro[3.3]heptane  
17 oxalate (150 mg, 0.79 mmol), 3-chloro-4-hydroxybenzaldehyde (160 mg, 1.02 mmol), TEA (310  
18 mg, 3.06 mmol) and HOAc (60 mg, 1.00 mmol) were dissolved in DCM (50 mL). Sodium  
19 triacetoxyborohydride (320 mg, 1.51 mmol) was added and the mixture stirred at rt for 2 h, then  
20 concentrated at reduced pressure. The residue was taken up in HCl (1M, 20mL) and EtOAc (20  
21 mL). The aqueous phase was basified with  $K_2CO_3$  to pH=8, then extracted with EtOAc (2x50 ml).  
22 The combined extracts were washed with brine, dried over  $Na_2SO_4$ , filtered and concentrated to  
23 give **41** (160 mg, 84 %).  $^1H$  NMR (500 MHz,  $CD_3OD$ )  $\delta$  7.22 (s, 1H), 7.03 (d,  $J = 7.7$  Hz, 1H),  
24 6.85 (d,  $J = 8.2$  Hz, 1H), 4.72 (s, 4H), 3.48 (s, 2H), 3.43 (s, 4H). LCMS (ES+)  $m/z$   $[M + H]^+$ :  
25 239.9.  
26  
27  
28  
29  
30  
31  
32  
33  
34  
35  
36  
37  
38

39 *1-(5-phenyl-1,3,4-oxadiazole-2-carbonyl)azetidin-3-yl 4-methylbenzenesulfonate (42)*. (3-  
40 hydroxyazetidin-1-yl)(5-phenyl-1,3,4-oxadiazol-2-yl)methanone (250 mg, 1.02 mmol) and TsCl  
41 (250 mg, 1.31 mmol) were dissolved in DCM (20 mL) and TEA (0.27 ml, 1.98 mmol) was  
42 added. The mixture was stirred at rt for 20 h, then evaporated. The residue was taken up in  
43 EtOAc (50 mL) and water (20 mL), the organic phase washed with brine, dried over  $Na_2SO_4$ ,  
44 filtered and concentrated to dryness. The solid residue was treated with diethyl ether (10 mL),  
45 filtered and washed with cold diethyl ether (5 mL) and air dried to give **42** (365 mg, 90 %).  $^1H$   
46 NMR (500 MHz,  $CDCl_3$ )  $\delta$  8.14 (d,  $J = 7.5$  Hz, 2H), 7.83 (d,  $J = 8.1$  Hz, 2H), 7.48 – 7.65 (m,  
47  
48  
49  
50  
51  
52  
53  
54  
55  
56  
57  
58  
59  
60

3H), 7.40 (d,  $J = 8.1$  Hz, 2H), 5.23 (s, 1H), 4.97 (s, 1H), 4.72 (d,  $J = 12$  Hz, 1H), 4.47 (s, 1H), 4.23 (d,  $J = 9.5$  Hz, 1H), 2.49 (s, 3H). LCMS (ES+)  $m/z$   $[M + H]^+$ : 400.0.

*(3-(4-(2-oxa-6-azaspiro[3.3]heptan-6-ylmethyl)-2-chlorophenoxy)azetidin-1-yl)(5-phenyl-1,3,4-oxadiazol-2-yl)methanone (7)*. **41** (130 mg, 0.54 mmol), **42** (220 mg, 0.55 mmol) and cesium carbonate (200 mg, 0.61 mmol) were mixed in a 5 mL microwave vial. DMF (5 mL) was added, the vial capped and the mixture was irradiated (130 °C for 30 min). The mixture was poured into EtOAc (30 mL) and water (15 mL). After separation the organic phase was washed with brine, dried over  $\text{Na}_2\text{SO}_4$ , filtered and concentrated at reduced pressure. The residue was suspended in toluene (20 mL) and concentrated again. This residue was flash chromatographed on a silica column (10 % TEA in EtOAc) to give the desired product **7** (130.0 mg, 51.3 %).  $^1\text{H}$  NMR (400 MHz,  $\text{CDCl}_3$ )  $\delta$  8.21 – 8.12 (m, 2H), 7.67 – 7.47 (m, 4H), 7.37 – 7.11 (m, 1H), 6.80 – 6.58 (m, 1H), 5.23 – 5.09 (m, 2H), 5.00 – 4.62 (m, 5H), 4.53 – 4.30 (m, 3H), 4.28 – 4.01 (m, 2H), 3.99 (s, 1H), 3.93 – 3.58 (m, 2H). HRMS calcd for  $\text{C}_{24}\text{H}_{24}\text{ClN}_4\text{O}_4^+$ ,  $[M + H]^+$ , 467.1486; found 467.1444.

**3-(4-(2-oxa-6-azaspiro[3.3]heptan-6-ylmethyl)-3-methylphenoxy)azetidin-1-yl)(5-(4-methoxyphenyl)-1,3,4-oxadiazol-2-yl)methanone (8)**.

*4-(1-(5-(4-methoxyphenyl)-1,3,4-oxadiazole-2-carbonyl)azetidin-3-yl)oxy-2-methylbenzaldehyde (43)*. 4-Hydroxy-2-methylbenzaldehyde (17.9 g, 131 mmol) and 1-(5-(4-methoxyphenyl)-1,3,4-oxadiazole-2-carbonyl)azetidin-3-yl methanesulfonate (52.7 g, 149 mmol) were mixed in DMA (250 mL). The mixture was heated to 95°C over 2 h, cesium carbonate (57 g, 175 mmol) was added at 70°C and the reaction was stirred at 95°C for 18 h. HOAc (11.3 mL, 197 mmol) was added to quench the reaction ( $\text{CO}_2$  formed) and the mixture was stirred at 30°C for 30 min, then most of the DMA was evaporated off at 60°C on a rotary evaporator. To the

1  
2  
3 residue, EtOAc (400 mL) was added and the organic phase washed with water (3x150 mL), then  
4  
5 EtOAc was evaporated off. To the residue, MeOH (500 mL) was added and the slurry was stirred  
6  
7 at 5°C overnight. The cold slurry was filtered, the filter cake washed with cold MeOH (2x100  
8  
9 mL) and the solid was dried under vacuum and heat (50°C) overnight to give **43** (34.6 g, 67%).  
10  
11 <sup>1</sup>H NMR (400 MHz, CDCl<sub>3</sub>) δ 10.14 (s, 1H), 8.09 (d, *J* = 8.9 Hz, 2H), 7.78 (d, *J* = 8.5 Hz, 1H),  
12  
13 7.02 (d, *J* = 8.9 Hz, 2H), 6.72 (dd, *J* = 2.4, 8.5 Hz, 1H), 6.64 (d, *J* = 2.1 Hz, 1H), 5.10 – 5.21 (m,  
14  
15 2H), 4.63 – 4.81 (m, 2H), 4.34 (dd, *J* = 2.2, 11.6 Hz, 1H), 3.89 (s, 3H), 2.66 (s, 3H).  
16  
17  
18

19  
20 *3-(4-(2-oxa-6-azaspiro[3.3]heptan-6-ylmethyl)-3-methylphenoxy)azetidin-1-yl)(5-(4-*  
21  
22 *methoxyphenyl)-1,3,4-oxadiazol-2-yl)methanone (8)*. **43** (1.3 g, 3.30 mmol) was dissolved in  
23  
24 DCM (40 mL). 2-oxa-6-azaspiro[3.3]heptane hemioxalate (0.953 g, 3.30 mmol), TEA (1.84 mL,  
25  
26 13.22 mmol) and sodium triacetoxyborohydride (2.10 g, 9.91 mmol) were added. THF (20 mL)  
27  
28 was added to improve solubility of the amine and the reaction was stirred at rt for 18 h. DCM (50  
29  
30 mL) and NaHCO<sub>3</sub> (sat., 50 mL) were added, the mixture shaken and the phases separated. The  
31  
32 aqueous phase was extracted with DCM (50 mL). The combined organic phases were dried with  
33  
34 a phase separator and evaporated in vacuo. The residue was purified by automated flash  
35  
36 chromatography on a Biotage® KP-SIL 100g column. A gradient of NH<sub>3</sub> in MeOH (2 M)/DCM  
37  
38 2:98 - 4:96 over 8 CV was used as mobile phase. The product was collected using the  
39  
40 wavelength 294 nm. The product fractions were pooled and evaporated in vacuo. The residue  
41  
42 was repurified by preparative HPLC on a XBridge C18 column (10 μm 250x50 ID mm) using a  
43  
44 gradient of 35-75% ACN in H<sub>2</sub>O/ACN/NH<sub>3</sub> 95/5/0.2 buffer over 20 min with a flow of 100  
45  
46 mL/min. The compounds were detected by UV at 290nm. The product fractions were freeze  
47  
48 dried to yield the product **8** (1.01 g, 63.8 %). <sup>1</sup>H NMR (400 MHz, CDCl<sub>3</sub>) δ 8.09 (d, *J* = 8.9 Hz,  
49  
50 2H), 7.13 (d, *J* = 8.3 Hz, 1H), 7.01 (d, *J* = 8.9 Hz, 2H), 6.61 – 6.5 (m, 2H), 5.16 – 4.99 (m, 2H),  
51  
52  
53  
54  
55  
56  
57  
58  
59  
60

1  
2  
3 4.79 – 4.67 (m, 5H), 4.67 – 4.58 (m, 1H), 4.36 – 4.23 (m, 1H), 3.88 (s, 3H), 3.46 (s, 2H), 3.37 (s,  
4  
5 4H), 2.28 (s, 3H). HRMS calcd for C<sub>26</sub>H<sub>29</sub>N<sub>4</sub>O<sub>5</sub><sup>+</sup>, [M + H]<sup>+</sup>, 477.2138; found 477.2137.

6  
7  
8  
9 **(3-(4-(2-oxa-6-azaspiro[3.3]heptan-6-ylmethyl)-2-methylphenoxy)azetidin-1-yl)(5-(4-**  
10  
11 **methoxyphenyl)-1,3,4-oxadiazol-2-yl)methanone (9).**

12  
13  
14 *4-(1-(5-(4-methoxyphenyl)-1,3,4-oxadiazole-2-carbonyl)azetidin-3-yl)oxy-3-methyl-*  
15  
16 *benzaldehyde (44)*. 4-Hydroxy-3-methylbenzaldehyde (1.7 g, 12.5 mmol) and 1-(5-(4-  
17  
18 methoxyphenyl)-1,3,4-oxadiazole-2-carbonyl)azetidin-3-yl methanesulfonate (4 g, 11.3 mmol)  
19  
20 were mixed in DMA (15 mL). Cesium carbonate (4.43 g, 13.6 mmol) was added and the mixture  
21  
22 was stirred at 97°C for 20 h, then cooled to rt. DCM (100 mL) and water (30 mL) were added,  
23  
24 the phases separated and the organic phase was washed with sat. K<sub>2</sub>CO<sub>3</sub> (30 mL) and water (30  
25  
26 mL), filtered through a phase separator and evaporated. Diethyl ether (20 mL) was added to give  
27  
28 a slurry. The solid was filtered off and washed with MeOH (10 mL) and diethyl ether (10 mL)  
29  
30 then dried under vacuum to give **44** (2.12 g, 48%). <sup>1</sup>H NMR (400 MHz, CDCl<sub>3</sub>) δ 9.89 (s, 1H),  
31  
32 8.10 (d, *J* = 8.8 Hz, 2H), 7.67 – 7.78 (m, 2H), 7.03 (d, *J* = 8.9 Hz, 2H), 6.61 (d, *J* = 8.3 Hz, 1H),  
33  
34 5.12 – 5.24 (m, 2H), 4.67 – 4.85 (m, 2H), 4.32 – 4.41 (m, 1H), 3.89 (s, 3H), 2.32 (s, 3H). LCMS  
35  
36 (ES<sup>+</sup>) *m/z* [M + H]<sup>+</sup>: 394.

37  
38  
39  
40  
41  
42 *(3-(4-(2-oxa-6-azaspiro[3.3]heptan-6-ylmethyl)-2-methylphenoxy)azetidin-1-yl)(5-(4-*  
43  
44 *methoxyphenyl)-1,3,4-oxadiazol-2-yl)methanone (9)*. **44** (2.11 g, 5.36 mmol) was suspended in  
45  
46 DCM (30 mL). 2-oxa-6-azaspiro[3.3]heptane hemioxalate (0.812 g, 5.63 mmol), TEA (0.82 mL,  
47  
48 5.9 mmol) and then sodium triacetoxyhydroborate (2.27 g, 10.7 mmol) were added. The mixture  
49  
50 was stirred at rt overnight. DCM (100 mL) and NaHCO<sub>3</sub> (sat. 20 mL) were added and the two  
51  
52 phases separated by using a phase separator. The organic phase was evaporated to dryness and  
53  
54 the residue was purified by Si column chromatography, eluting with ammonia in MeOH  
55  
56  
57  
58  
59  
60

(2M)/DCM (1:99, 2:98). The obtained product (1.91 g) was re-crystallized in EtOAc to give **9** (1.67 g, 65%). <sup>1</sup>H NMR (400 MHz, CDCl<sub>3</sub>) δ 8.09 (d, *J* = 8.9 Hz, 2H), 7.09 – 6.95 (m, 4H), 6.42 (d, *J* = 8.2 Hz, 1H), 5.17 – 4.99 (m, 2H), 4.78 – 4.68 (m, 5H), 4.68 – 4.58 (m, 1H), 4.36 – 4.27 (m, 1H), 3.88 (s, 3H), 3.43 (s, 2H), 3.34 (s, 4H), 2.22 (s, 3H). HRMS calcd for C<sub>26</sub>H<sub>29</sub>N<sub>4</sub>O<sub>5</sub><sup>+</sup>, [M + H]<sup>+</sup>, 477.2138; found 477.2149.

**(3-(4-(2-oxa-6-azaspiro[3.3]heptan-6-ylmethyl)-3-methoxyphenoxy)azetid-1-yl)(5-(4-(difluoromethyl)phenyl)-1,3,4-oxadiazol-2-yl)methanone (10).**

*3-methoxy-4-(2-oxa-6-azaspiro[3.3]heptan-6-ylmethyl)phenol (45)*. 4-Hydroxy-2-methoxybenzaldehyde (0.31 g, 2.05 mmol), 2-oxa-6-azaspiro[3.3]heptane hemioxalate (0.44 g, 1.54 mmol) and TEA (1.14 mL, 8.20 mmol) were mixed in DCM (8 mL) and stirred for 30 min. Sodium triacetoxyhydroborate (0.87 g, 4.10 mmol) was added and the reaction stirred for 24 h. The reaction mixture was diluted with DCM (50 mL) and 8% NaHCO<sub>3</sub> (85 mL) was added. The organic phase was separated and the aqueous layer extracted with DCM (2x50 mL). The organic phases were pooled, filtered through a phase separator and evaporated to provide **45** (207 mg, 43%). LCMS (ES+) *m/z* [M + H]<sup>+</sup>: 236.2.

*1-(5-(4-(difluoromethyl)phenyl)-1,3,4-oxadiazole-2-carbonyl)azetid-3-yl 4-methylbenzenesulfonate (46)*. To **37** (4.82 g, 16.1 mmol) in DCM (100 mL) were added TsCl (4.35 g, 22.8 mmol) and N,N-dimethylpyridin-4-amine (2.89 g, 23.7 mmol) and the reaction was stirred at rt for 20 h. 0.5 M KHSO<sub>4</sub> (aq, 100 mL) was added and the organic phase was washed with 8% NaHCO<sub>3</sub> (aq, 100 mL), dried over a phase separator and evaporated to give **46** (7.24 g, 99%). <sup>1</sup>H NMR (400 MHz, CDCl<sub>3</sub>) δ 8.22 (d, *J* = 8.1 Hz, 2H), 7.81 (d, *J* = 8.3 Hz, 2H), 7.67 (d, *J* = 8.3 Hz, 2H), 7.39 (d, *J* = 8.2 Hz, 2H), 6.70 (t, *J* = 56 Hz, 1H), 5.17 – 5.26 (m, 1H), 4.94 –

5.02 (m, 1H), 4.67 – 4.76 (m, 1H), 4.42 – 4.51 (m, 1H), 4.18 – 4.26 (m, 1H), 2.48 (s, 3H). LCMS (ES+)  $m/z$   $[M + H]^+$ : 450.1.

*(3-(4-(2-oxa-6-azaspiro[3.3]heptan-6-ylmethyl)-3-methoxyphenoxy)azetidin-1-yl)(5-(4-(difluoromethyl)phenyl)-1,3,4-oxadiazol-2-yl)methanone (10)*. **46** (0.345 g, 0.65 mmol), **45** (0.211 g, 0.72 mmol) and cesium carbonate (0.213 g, 0.65 mmol) were mixed in DMA (3 mL) and the mixture heated in a microwave (160°C for 15 min). DCM (10 ml) and then NaHCO<sub>3</sub> (sat. 5 ml) were added. The two phases were separated by using a phase separator and the organic phase was evaporated to dryness. The product was purified by preparative HPLC eluting with a gradient of ACN (5-95%) in 0.2% ammonia buffer to afford **10** (35 mg, 11%). <sup>1</sup>H NMR (400 MHz, CDCl<sub>3</sub>)  $\delta$  8.27 (d,  $J$  = 8.3 Hz, 2H), 7.70 (d,  $J$  = 8.2 Hz, 2H), 6.88 – 6.57 (m, 4H), 5.15 – 5.04 (m, 2H), 4.88 – 4.81 (m, 1H), 4.76 (s, 4H), 4.68 – 4.60 (m, 1H), 4.47 – 4.39 (m, 1H), 3.89 (s, 3H), 3.50 (s, 2H), 3.38 (s, 4H). HRMS calcd for C<sub>26</sub>H<sub>26</sub>F<sub>2</sub>N<sub>4</sub>O<sub>5</sub><sup>+</sup>, (M)<sup>+</sup>, 513.1949; found 513.1945.

*(3-(4-(2-oxa-6-azaspiro[3.3]heptan-6-ylmethyl)-2-methoxyphenoxy)azetidin-1-yl)(5-(4-(difluoromethyl)phenyl)-1,3,4-oxadiazol-2-yl)methanone (11)*.

*2-methoxy-4-(2-oxa-6-azaspiro[3.3]heptan-6-ylmethyl)phenol (47)*. 4-Hydroxy-3-methoxybenzaldehyde (0.28 mL, 1.97 mmol), 2-oxa-6-azaspiro[3.3]heptane hemioxalate (0.43 g, 1.48 mmol) and TEA (1.09 mL, 7.89 mmol) were mixed in DCM (8 mL) and stirred for 30 min. Sodium triacetoxyhydroborate (0.836 g, 3.94 mmol) was added and the reaction stirred for 2 days. The reaction mixture was diluted with DCM (50 mL) and 8% NaHCO<sub>3</sub> (850 mL) was added. The phases were separated and the aqueous layer extracted with DCM (2 x 50 mL). The organic phases were pooled, passed over a phase separator and the solvent removed in vacuo to

1  
2  
3 provide **47** (0.51 g, 111%). <sup>1</sup>H NMR (400 MHz, CDCl<sub>3</sub>) δ 6.77 – 6.84 (m, 2H), 6.70 (dd, *J* = 1.6,  
4 8.0 Hz, 1H), 4.73 (s, 4H), 3.86 (s, 3H), 3.47 (s, 2H), 3.37 (s, 4H).

5  
6  
7 *(3-(4-(2-oxa-6-azaspiro[3.3]heptan-6-ylmethyl)-2-methoxyphenoxy)azetid-1-yl)(5-(4-*

8 *(difluoromethyl)phenyl)-1,3,4-oxadiazol-2-yl)methanone (11)*. **46** (0.345 g, 0.65 mmol), **47**

9  
10 (0.207 g, 0.70 mmol) and cesium carbonate (0.229 g, 0.70 mmol) were mixed in DMA (3 mL)

11  
12 and the mixture heated in a microwave (160°C for 15 min). DCM (10 mL) and then NaHCO<sub>3</sub>

13  
14 (sat. 5 mL) were added. The two phases were separated by using a phase separator and the

15  
16 organic phase was evaporated to dryness. The product was purified by preparative HPLC eluting

17  
18 with a gradient of ACN (5-95%) in 0.2% ammonia buffer to afford **11** (20 mg, 6%). <sup>1</sup>H NMR

19  
20 (400 MHz, CDCl<sub>3</sub>) δ 8.26 (d, *J* = 8.4 Hz, 2H), 7.69 (d, *J* = 8.2 Hz, 2H), 7.12 (d, *J* = 8.2 Hz, 1H),

21  
22 6.72 (t, *J* = 56 Hz, 1H), 6.40 (d, *J* = 2.3 Hz, 1H), 6.22 (dd, *J* = 8.2, 2.3 Hz, 1H), 5.17 – 5.03 (m,

23  
24 2H), 4.79 – 4.70 (m, 5H), 4.69 – 4.61 (m, 1H), 4.37 – 4.30 (m, 1H), 3.80 (s, 3H), 3.51 (s, 2H),

25  
26 3.42 (s, 4H). HRMS calcd for C<sub>26</sub>H<sub>26</sub>F<sub>2</sub>N<sub>4</sub>O<sub>5</sub><sup>+</sup>, (M)<sup>+</sup>, 513.1949; found 513.1947.

27  
28  
29 **(3-(4-((3,3-bis(hydroxymethyl)azetid-1-yl)methyl)phenoxy)azetid-1-yl)(5-(4-**

30  
31 **methoxyphenyl)-1,3,4-oxadiazol-2-yl)methanone (12)**.

32  
33  
34 *(3-(4-(2-oxa-6-azaspiro[3.3]heptan-6-ylmethyl)phenoxy)azetid-1-yl)(5-(4-methoxyphenyl)-*

35  
36 *1,3,4-oxadiazol-2-yl)methanone 1* (200 mg, 0.43 mmol) was dissolved in 1,4-dioxane (8 mL)

37  
38 and H<sub>2</sub>SO<sub>4</sub> (0.41 mL, 0.13 mmol) was added at rt. Another portion of dioxane (4 mL) was added

39  
40 and the reaction mixture was stirred at rt for 1h, then at 75°C for 1h. The mixture was diluted

41  
42 with EtOAc (5 mL) and NaHCO<sub>3</sub> (aq, 5%, 2mL), the organic phase was dried and solvents were

43  
44 evaporated. The residue was purified by preparative HPLC eluting with a gradient of ACN (20-

45  
46 60%) in 0.2% ammonia buffer to afford **12** (30 mg, 14%). <sup>1</sup>H NMR (400 MHz, CDCl<sub>3</sub>) δ 8.03 –

47  
48 8.17 (m, 2H), 7.23 (d, 2H), 7 – 7.06 (m, 2H), 6.73 (d, 2H), 5.02 – 5.17 (m, 2H), 4.71 – 4.78 (m,

1  
2  
3 1H), 4.6 – 4.68 (m, 1H), 4.25 – 4.38 (m, 1H), 3.90 (s, 3H), 3.83 (s, 4H), 3.60 (s, 2H), 3.13 (s,  
4  
5 4H). HRMS calcd for C<sub>25</sub>H<sub>29</sub>N<sub>4</sub>O<sub>6</sub><sup>+</sup>, [M + H]<sup>+</sup>, 481.2087; found 481.2076.

6  
7  
8  
9 **(3-(4-(((3-(hydroxymethyl)oxetan-3-yl)methyl)amino)methyl)phenoxy)azetid-1-yl)(5-(4-**  
10  
11 **methoxyphenyl)-1,3,4-oxadiazol-2-yl)methanone (13).**

12  
13  
14 (3-(aminomethyl)oxetan-3-yl)methanol (93 mg, 0.79 mmol) and 4-((1-(5-(4-methoxyphenyl)-  
15  
16 1,3,4-oxadiazole-2-carbonyl)azetid-3-yl)oxy)benzaldehyde (200 mg, 0.53 mmol) were mixed  
17  
18 in DCM (2 mL) and MeOH (1 mL) and stirred at rt for 1 h. HOAc (0.060 mL, 1.05 mmol) and  
19  
20 sodium triacetoxyborohydride (223 mg, 1.05 mmol) were added and the reaction stirred at rt  
21  
22 overnight. DCM (5 mL) and NaHCO<sub>3</sub> (sat. 5 mL) were added, the mixture stirred, filtered  
23  
24 through a phase separator and evaporated. The residue was purified by preparative HPLC eluting  
25  
26 with a gradient of ACN (5-95%) in 0.2% ammonia buffer to afford **13** (164 mg, 65%). <sup>1</sup>H NMR  
27  
28 (400 MHz, CDCl<sub>3</sub>) δ 8.06 – 8.13 (m, 2H), 7.24 (d, *J* = 8.6 Hz, 2H), 6.98 – 7.05 (m, 2H), 6.72 –  
29  
30 6.78 (m, 2H), 5.01 – 5.15 (m, 2H), 4.69 – 4.77 (m, 1H), 4.59 – 4.68 (m, 1H), 4.39 – 4.48 (m,  
31  
32 4H), 4.27 – 4.35 (m, 1H), 4.01 (s, 2H), 3.89 (s, 3H), 3.77 (s, 2H), 3.15 (s, 2H), 2.61 (s, 1H).  
33  
34 HRMS calcd for C<sub>25</sub>H<sub>29</sub>N<sub>4</sub>O<sub>6</sub><sup>+</sup>, [M + H]<sup>+</sup>, 481.2087; found 481.2076.

35  
36  
37  
38  
39  
40 **(3-(4-(2-oxa-6-azaspiro[3.5]nonan-6-ylmethyl)-3-methylphenoxy)azetid-1-yl)(5-phenyl-**  
41  
42 **1,3,4-oxadiazol-2-yl)methanone (15).**

43  
44  
45 **43** (0.1 g, 0.28 mmol) and 2-oxa-6-azaspiro[3.5]nonane (0.042 g, 0.33 mmol) were mixed in  
46  
47 DCM (3 mL). TEA (0.057 mL, 0.41 mmol) was added, and then sodium triacetoxyhydroborate  
48  
49 (0.087 g, 0.41 mmol) was added. The mixture was stirred at rt overnight. DCM (10 mL) and  
50  
51 NaHCO<sub>3</sub>(sat. 2 ml) were added, the phases separated by using a phase separator and the organic  
52  
53 phase evaporated to dryness. The product was purified by preparative HPLC eluting with a  
54  
55  
56  
57  
58  
59  
60

1  
2  
3 gradient of ACN (5-95%) in 0.2% ammonia buffer to afford **15** (86 mg, 66%). <sup>1</sup>H NMR (600  
4 MHz, DMSO-*d*<sub>6</sub>) δ 8.07 – 8.01 (m, 2H), 7.69 – 7.64 (m, 1H), 7.64 – 7.58 (m, 2H), 7.11 (d, *J* =  
5 8.3 Hz, 1H), 6.70 (d, *J* = 2.6 Hz, 1H), 6.63 (dd, *J* = 8.2, 2.7 Hz, 1H), 5.14 – 5.03 (m, 2H), 4.63 –  
6 4.57 (m, 1H), 4.19 (d, *J* = 5.7 Hz, 2H), 4.10 (d, *J* = 5.7 Hz, 2H), 4.06 (dd, *J* = 11.3, 2.3 Hz, 1H),  
7 3.34 (s, 2H), 3.28 (s, 2H), 2.28 (s, 3H), 2.19 (br, 2H), 1.59 (br, 2H), 1.41 – 1.29 (m, 2H). HRMS  
8  
9  
10 calcd for C<sub>27</sub>H<sub>31</sub>N<sub>4</sub>O<sub>4</sub><sup>+</sup> [M + H]<sup>+</sup>, 475.2345; found 475.2375.  
11  
12  
13  
14  
15

16  
17  
18 **(3-(4-(2-oxa-5-azaspiro[3.4]octan-5-ylmethyl)-3-methoxyphenoxy)azetid-1-yl)(5-phenyl-**  
19  
20 **1,3,4-oxadiazol-2-yl)methanone (17).**  
21  
22

23 *2-methoxy-4-(1-(5-phenyl-1,3,4-oxadiazole-2-carbonyl)azetid-3-yloxy)benzaldehyde (48).* 4-  
24 Hydroxy-2-methoxybenzaldehyde (0.49 g, 3.25 mmol) and 1-(5-phenyl-1,3,4-oxadiazole-2-  
25 carbonyl)azetid-3-yl methanesulfonate (1 g, 3.09 mmol) were mixed in DMA (10 mL). Cesium  
26 carbonate (1.21 g, 3.71 mmol) was added. The mixture was stirred at 94°C overnight, then cooled  
27 to rt. EtOAc (50 mL) was added and the mixture was washed with water (20 mL), sat. K<sub>2</sub>CO<sub>3</sub>  
28 (10 mL), water (10 mL) and brine (10 mL), dried with MgSO<sub>4</sub> and evaporated. MeOH (15 mL)  
29 was added to the residue, the slurry was stirred and then filtered and the solid product was  
30 washed with MeOH (10 mL) then dried under vacuum to give **48** (0.72 g, 61%). <sup>1</sup>H NMR (400  
31 MHz, CDCl<sub>3</sub>) δ 10.32 (s, 1H), 8.12 – 8.21 (m, 2H), 7.84 (d, *J* = 8.6 Hz, 1H), 7.49 – 7.65 (m, 3H),  
32 6.43 (d, *J* = 2.1 Hz, 1H), 6.35 (dd, *J* = 2.0, 8.6 Hz, 1H), 5.11 – 5.22 (m, 2H), 4.61 – 4.84 (m, 2H),  
33 4.31 – 4.41 (m, 1H), 3.92 (s, 3H). LCMS (ES<sup>+</sup>) *m/z* [M + H]<sup>+</sup>: 380.2.  
34  
35  
36  
37  
38  
39  
40  
41  
42  
43  
44  
45  
46  
47  
48

49 *(3-(4-(2-oxa-5-azaspiro[3.4]octan-5-ylmethyl)-3-methoxyphenoxy)azetid-1-yl)(5-phenyl-1,3,4-*  
50 *oxadiazol-2-yl)methanone (17).* **48** (0.111 g, 0.34 mmol) and 2-oxa-5-azaspiro[3.4]octane  
51 hydrochloride (0.13 g, 0.34 mmol) were mixed in DCM (2 mL). TEA (0.1 mL, 0.72 mmol) and  
52  
53  
54  
55  
56  
57  
58  
59  
60

sodium triacetoxyhydroborate (0.145 g, 0.69 mmol) were added and the reaction was stirred at rt overnight. DCM (10 mL) and NaHCO<sub>3</sub> (sat. 3 mL) were added, the mixture shaken, filtered through a phase separator and evaporated. The residue was purified by preparative HPLC eluting with a gradient of ACN (5-95%) in 0.2% ammonia buffer to afford **17** (113 mg, 69%). <sup>1</sup>H NMR (600 MHz, DMSO-*d*<sub>6</sub>) δ 8.12 – 8.05 (m, 2H), 7.74 – 7.62 (m, 3H), 7.20 (d, *J* = 8.3 Hz, 1H), 6.54 (d, *J* = 2.4 Hz, 1H), 6.42 (dd, *J* = 8.2, 2.4 Hz, 1H), 5.22 – 5.15 (m, 1H), 5.13-5.07 (m, 1H), 4.79 (d, *J* = 6.6 Hz, 2H), 4.67 – 4.61 (m, 1H), 4.58 – 4.53 (m, 1H), 4.44 (d, *J* = 6.6 Hz, 2H), 4.13 – 4.07 (m, 1H), 3.88 (s, 2H), 3.81 (s, 3H), 2.59 – 2.54 (m, 2H), 2.14 – 2.06 (m, 2H), 1.67 – 1.58 (m, 2H). HRMS calcd for C<sub>26</sub>H<sub>29</sub>N<sub>4</sub>O<sub>5</sub><sup>+</sup>, [M + H]<sup>+</sup>, 477.2138; found 477.2165.

**(3-(4-(2-oxa-5-azaspiro[3.4]octan-5-ylmethyl)-2-methoxyphenoxy)azetid-1-yl)(5-phenyl-1,3,4-oxadiazol-2-yl)methanone (18).**

*3-methoxy-4-(1-(5-phenyl-1,3,4-oxadiazole-2-carbonyl)azetid-3-yloxy)benzaldehyde (49).*

Synthesized in an analogous way to **48** from 4-Hydroxy-3-methoxybenzaldehyde (0.49 g, 3.25 mmol) and 1-(5-phenyl-1,3,4-oxadiazole-2-carbonyl)azetid-3-yl methanesulfonate (1.0 g, 3.09 mmol), to give **49** (0.95 g, 81%). <sup>1</sup>H NMR (400 MHz, CDCl<sub>3</sub>) δ 9.89 (s, 1H), 8.12 – 8.20 (m, 2H), 7.50 – 7.64 (m, 3H), 7.38 – 7.50 (m, 2H), 6.73 (d, *J* = 8.0 Hz, 1H), 5.12 – 5.24 (m, 2H), 4.87 (q, *J* = 6.6 Hz, 1H), 4.71 (dd, *J* = 5.7, 12.4 Hz, 1H), 4.45 (dd, *J* = 2.5, 11.5 Hz, 1H), 3.96 (s, 3H). LCMS (ES<sup>+</sup>) *m/z* [M + H]<sup>+</sup>: 380.2.

*(3-(4-(2-oxa-5-azaspiro[3.4]octan-5-ylmethyl)-2-methoxyphenoxy)azetid-1-yl)(5-phenyl-1,3,4-oxadiazol-2-yl)methanone (18).* 2-Oxa-5-azaspiro[3.4]octane hydrochloride (0.111 g, 0.34 mmol) and **49** (0.13 g, 0.34 mmol) were mixed in DCM (2 mL). TEA (0.1 mL, 0.72 mmol) and sodium triacetoxyhydroborate (0.145 g, 0.69 mmol) were added and the mixture was stirred at rt

overnight. DCM (10 mL) and NaHCO<sub>3</sub> (sat. 3 mL) were added, the mixture filtered through a phase separator and evaporated. The residue was purified by preparative HPLC eluting with a gradient of ACN (5-95%) in 0.2% ammonia buffer. The product was further purified by automated flash chromatography on a 10 g Si column. 3% of NH<sub>3</sub> (2M) in MeOH/EtOAc over 20 CV was used as mobile phase. The product was collected using the wavelength 274 nm to afford **18** (90 mg, 55%). <sup>1</sup>H NMR (400 MHz, CDCl<sub>3</sub>) δ 8.17 (d, *J* = 7.1 Hz, 2H), 7.63 – 7.45 (m, 3H), 6.95 (s, 1H), 6.87 (d, *J* = 8.1 Hz, 1H), 6.63 (d, *J* = 8.1 Hz, 1H), 5.15 – 5.03 (m, 2H), 4.90 (d, *J* = 6.7 Hz, 2H), 4.87 – 4.81 (m, 1H), 4.67 – 4.60 (m, 1H), 4.57 (d, *J* = 6.7 Hz, 2H), 4.46 – 4.39 (m, 1H), 3.97 (s, 2H), 3.89 (s, 3H), 2.60 (t, *J* = 7.0 Hz, 2H), 2.25 – 2.17 (m, 2H), 1.71 (p, *J* = 7.1, 7.0 Hz, 2H). HRMS calcd for C<sub>26</sub>H<sub>29</sub>N<sub>4</sub>O<sub>5</sub><sup>+</sup>, [M + H]<sup>+</sup>, 477.2138; found 477.2128.

**(3-(4-(2-oxa-5-azaspiro[3.4]octan-5-ylmethyl)-3-methoxyphenoxy)azetid-1-yl)(5-(4-(difluoromethyl)phenyl)-1,3,4-oxadiazol-2-yl)methanone (19).**

*4-(1-(5-(4-(difluoromethyl)phenyl)-1,3,4-oxadiazole-2-carbonyl)azetid-3-yl)oxy-2-methoxybenzaldehyde (50)*. Synthesized in an analogous way to **48** from 4-Hydroxy-2-methoxybenzaldehyde (0.14 g, 0.93 mmol) and **46** (0.4 g, 0.89 mmol), to give **50** (0.23 g, 59%). <sup>1</sup>H NMR (400 MHz, CDCl<sub>3</sub>) δ 10.32 (s, 1H), 8.27 (d, *J* = 8.4 Hz, 2H), 7.84 (d, *J* = 8.6 Hz, 1H), 7.70 (d, *J* = 8.2 Hz, 2H), 6.72 (t, *J* = 56 Hz, 1H), 6.44 (d, *J* = 2.2 Hz, 1H), 6.35 (dd, *J* = 1.9, 8.5 Hz, 1H), 5.12 – 5.23 (m, 2H), 4.65 – 4.86 (m, 2H), 4.32 – 4.40 (m, 1H), 3.92 (s, 3H). LCMS (ES+) *m/z* [M + H]<sup>+</sup>: 430.2.

*(3-(4-(2-oxa-5-azaspiro[3.4]octan-5-ylmethyl)-3-methoxyphenoxy)azetid-1-yl)(5-(4-(difluoromethyl)phenyl)-1,3,4-oxadiazol-2-yl)methanone (19)*. 2-Oxa-5-azaspiro[3.4]octane hydrochloride (0.11 g, 0.34 mmol) and **50** (0.146 g, 0.34 mmol) were mixed in DCM (2 mL). TEA (0.1 mL, 0.72 mmol) and sodium triacetoxhydroborate (0.145 g, 0.68 mmol) were added.

The mixture was stirred at rt overnight. DCM (10 mL) and NaHCO<sub>3</sub> (sat. 3 mL) were added, the mixture shaken, filtered through a phase separator and evaporated. The residue was purified by preparative HPLC eluting with a gradient of ACN (5-95%) in 0.2% ammonia buffer to afford **19** (119 mg, 67%). <sup>1</sup>H NMR (600 MHz, DMSO-*d*<sub>6</sub>) δ 8.23 (d, *J* = 8.3 Hz, 2H), 7.85 (d, *J* = 8.2 Hz, 2H), 7.32 – 7.05 (m, 2H), 6.54 (d, *J* = 2.2 Hz, 1H), 6.42 (dd, *J* = 8.2, 2.2 Hz, 1H), 5.23 – 5.15 (m, 1H), 5.14 – 5.07 (m, 1H), 4.79 (d, *J* = 6.5 Hz, 2H), 4.72 – 4.60 (m, 1H), 4.60 – 4.53 (m, 1H), 4.44 (d, *J* = 6.5 Hz, 2H), 4.11 (dd, *J* = 11.3, 2.3 Hz, 1H), 3.88 (s, 2H), 3.81 (s, 3H), 2.58 – 2.55 (m, 2H), 2.13 – 2.04 (m, 2H), 1.69 – 1.57 (m, 2H). HRMS calcd for C<sub>27</sub>H<sub>29</sub>F<sub>2</sub>N<sub>4</sub>O<sub>5</sub><sup>+</sup>, [M + H]<sup>+</sup>, 527.2106; found 527.2113.

**(3-(4-(2-oxa-5-azaspiro[3.4]octan-5-ylmethyl)-2-methoxyphenoxy)azetidino-1-yl)(5-(4-(difluoromethyl)phenyl)-1,3,4-oxadiazol-2-yl)methanone (20).**

*4-(1-(5-(4-(difluoromethyl)phenyl)-1,3,4-oxadiazole-2-carbonyl)azetidino-3-yloxy)-3-methoxybenzaldehyde (51)*. Synthesized in an analogous way to **48** from 4-Hydroxy-3-methoxybenzaldehyde (0.14 g, 0.93 mmol) and **46** (0.4 g, 0.89 mmol), to give **51** (0.23 g, 59%). <sup>1</sup>H NMR (400 MHz, CDCl<sub>3</sub>) δ 9.89 (s, 1H), 8.27 (d, *J* = 8.5 Hz, 2H), 7.70 (d, *J* = 8.2 Hz, 2H), 7.41 – 7.51 (m, 2H), 6.52 – 6.89 (m, 2H), 5.15 – 5.24 (m, 2H), 4.83 – 4.93 (m, 1H), 4.71 (dd, *J* = 6.2, 13.3 Hz, 1H), 4.46 (dd, *J* = 2.8, 11.4 Hz, 1H), 3.96 (s, 3H). LCMS (ES<sup>+</sup>) *m/z* [M + H]<sup>+</sup>: 430.2.

*(3-(4-(2-oxa-5-azaspiro[3.4]octan-5-ylmethyl)-2-methoxyphenoxy)azetidino-1-yl)(5-(4-(difluoromethyl)phenyl)-1,3,4-oxadiazol-2-yl)methanone (20)*. 2-Oxa-5-azaspiro[3.4]octane hydrochloride (0.11 g, 0.34 mmol) and **51** (0.146 g, 0.34 mmol) were mixed in DCM (2 mL). TEA (0.1 mL, 0.72 mmol) was added and then sodium triacetoxyhydroborate (0.144 g, 0.68

mmol) was added. The reaction was stirred at rt overnight. DCM (10 mL) and NaHCO<sub>3</sub> (sat. 3 mL) were added, the mixture stirred, filtered through a phase separator and evaporated. The residue was purified by preparative HPLC eluting with a gradient of ACN (5-95%) in 0.2% ammonia buffer to afford **20** (112 mg, 63%). <sup>1</sup>H NMR (400 MHz, CDCl<sub>3</sub>) δ 8.27 (d, *J* = 8.3 Hz, 2H), 7.70 (d, *J* = 8.3 Hz, 2H), 6.96 (s, 1H), 6.91 – 6.56 (m, 3H), 5.16 – 5.05 (m, 2H), 4.91 (d, *J* = 6.7 Hz, 2H), 4.89 – 4.82 (m, 1H), 4.68 – 4.61 (m, 1H), 4.58 (d, *J* = 6.7 Hz, 2H), 4.48 – 4.40 (m, 1H), 3.99 (s, 2H), 3.90 (s, 3H), 2.64 – 2.57 (m, 2H), 2.26 – 2.19 (m, 2H), 1.77 – 1.68 (m, 2H). HRMS calcd for C<sub>27</sub>H<sub>29</sub>F<sub>2</sub>N<sub>4</sub>O<sub>5</sub><sup>+</sup>, [M + H]<sup>+</sup>, 527.2106; found 527.2128.

**(3-(4-(6-oxa-3-azabicyclo[3.1.1]heptan-3-ylmethyl)phenoxy)azetidin-1-yl)(5-(4-methoxyphenyl)-1,3,4-oxadiazol-2-yl)methanone (23).**

6-Oxa-3-azabicyclo[3.1.1]heptane (107 mg, 0.40 mmol) and TEA (44 mg, 0.43 mmol) were mixed in DCM (3 mL) and THF(1 ml) and 4-(1-(5-(4-methoxyphenyl)-1,3,4-oxadiazole-2-carbonyl)azetidin-3-yloxy)benzaldehyde (150 mg, 0.40 mmol) was added. Molecular sieves 3 Å were added and the mixture was stirred at rt for 40 min. HOAc (48 mg, 0.79 mmol) and sodium triacetoxyborohydride (101 mg, 0.47 mmol) were added and the reaction was stirred over night at rt. DCM (15 mL) and NaOH (2M, 10 mL) were added, the mixture stirred, filtered through a phase separator and evaporated. Upon trying to dissolve in DMSO, a precipitate was formed. This was filtered off to afford **23** (55 mg, 30%). <sup>1</sup>H NMR (500 MHz, CDCl<sub>3</sub>) δ 8.13 – 8.07 (m, 2H), 7.30 (d, *J* = 8.6 Hz, 2H), 7.05 – 7.00 (m, 2H), 6.74 (d, *J* = 8.6 Hz, 2H), 5.15 – 5.03 (m, 2H), 4.75 (ddd, *J* = 11.0, 3.6, 1.5 Hz, 1H), 4.64 (ddd, *J* = 11.4, 6.3, 1.6 Hz, 1H), 4.49 (d, *J* = 6.1 Hz, 2H), 4.36 – 4.30 (m, 1H), 3.89 (s, 3H), 3.71 (s, 2H), 3.07 – 2.96 (m, 3H), 2.79 (d, *J* = 11.0 Hz, 2H), 2.41 (d, *J* = 7.8 Hz, 1H). HRMS calcd for C<sub>25</sub>H<sub>27</sub>N<sub>4</sub>O<sub>5</sub><sup>+</sup>, [M + H]<sup>+</sup>, 463.1981; found 463.1967.

**6-(4-methoxybenzyl)-2-oxa-6-azaspiro[3.3]heptane (24).**

4-Methoxybenzaldehyde (0.061 mL, 0.5 mmol), 2-oxa-6-azaspiro[3.3]heptane oxalate (142 mg, 0.75 mmol), and TEA (0.139 mL, 1.00 mmol) were mixed in DCM (2 mL). The mixture was stirred at rt for 15 min, then sodium triacetoxyborohydride (212 mg, 1.00 mmol) was added and the reaction was stirred at rt overnight. More DCM (5 mL) and NaHCO<sub>3</sub> (sat. 5 mL) were added, the mixture stirred for 15 min, filtered through a phase separator and evaporated. The residue was purified by preparative HPLC eluting with a gradient of ACN (5-95%) in 0.2% ammonia buffer to afford **24** (6.2 mg, 5.7%). <sup>1</sup>H NMR (400 MHz, CDCl<sub>3</sub>) δ 7.15 (d, *J* = 8.7 Hz, 2H), 6.84 (d, *J* = 8.7 Hz, 2H), 4.73 (s, 4H), 3.79 (s, 3H), 3.47 (s, 2H), 3.35 (s, 4H). HRMS calcd for C<sub>13</sub>H<sub>18</sub>NO<sub>2</sub><sup>+</sup>, [M + H]<sup>+</sup>, 220.1337; found 220.1342.

**6-(4-methoxybenzyl)-2-oxa-6-azaspiro[3.5]nonane (25).**

4-Methoxybenzaldehyde (0.061 mL, 0.5 mmol), 2-oxa-6-azaspiro[3.5]nonane (95 mg, 0.75 mmol) and HOAc (0.057 mL, 1.00 mmol) were mixed in DCM (2 mL). The mixture was stirred at rt for 15 min, then sodium triacetoxyborohydride (212 mg, 1.00 mmol) was added and the reaction was stirred at rt overnight. More DCM (5 mL) and NaHCO<sub>3</sub> (sat. 5 mL) were added, the mixture stirred for 15 min, filtered through a phase separator and evaporated. The residue was purified by preparative HPLC eluting with a gradient of ACN (5-95%) in 0.2% ammonia buffer to afford **25** (46 mg, 37%). <sup>1</sup>H NMR (400 MHz, CDCl<sub>3</sub>) δ 7.28 (d, *J* = 8.7 Hz, 2H), 6.95 – 6.89 (m, 2H), 4.45 – 4.37 (m, 4H), 3.87 (s, 3H), 3.51 (s, 2H), 2.57 (br, 2H), 2.37 (br, 2H), 1.75 (br, 2H), 1.64 – 1.52 (m, 2H). HRMS calcd for C<sub>15</sub>H<sub>22</sub>NO<sub>2</sub><sup>+</sup>, [M + H]<sup>+</sup>, 248.1650; found 248.1646.

**7-(4-methoxybenzyl)-2-oxa-7-azaspiro[3.5]nonane (26).**

4-Methoxybenzaldehyde (0.061 mL, 0.5 mmol), 2-oxa-7-azaspiro[3.5]nonane (95 mg, 0.75 mmol) and HOAc (0.057 mL, 1.00 mmol) were mixed in DCM (2 mL). The mixture was stirred at rt for 15 min, then sodium triacetoxyborohydride (212 mg, 1.00 mmol) was added and the reaction was stirred at rt overnight. More DCM (5 mL) and NaHCO<sub>3</sub> (sat. 5 mL) were added, the mixture stirred for 15 min, filtered through a phase separator and evaporated. The residue was purified by preparative HPLC eluting with a gradient of ACN (5-95%) in 0.2% ammonia buffer to afford **26** (47 mg, 38%). <sup>1</sup>H NMR (400 MHz, CDCl<sub>3</sub>) δ 7.32 – 7.24 (m, 2H), 6.98 – 6.88 (m, 2H), 4.47 (s, 4H), 3.88 (s, 3H), 3.46 (s, 2H), 2.37 (s, 4H), 2.01 – 1.87 (m, 4H). HRMS calcd for C<sub>15</sub>H<sub>22</sub>NO<sub>2</sub><sup>+</sup>, [M + H]<sup>+</sup>, 248.1650; found 248.1664.

**5-(4-methoxybenzyl)-2-oxa-5-azaspiro[3.4]octane (27).**

4-Methoxybenzaldehyde (0.061 mL, 0.5 mmol), 2-oxa-5-azaspiro[3.4]octane 2,2,2-trifluoroacetate (170 mg, 0.75 mmol) and HOAc (0.057 mL, 1.00 mmol) were mixed in DCM (2 mL). The mixture was stirred at rt for 15 min, then sodium triacetoxyborohydride (212 mg, 1.00 mmol) was added and the reaction was stirred at rt overnight. More DCM (5 mL) and NaHCO<sub>3</sub> (sat. 5 mL) were added, the mixture stirred for 15 min, filtered through a phase separator and evaporated. The residue was purified by preparative HPLC eluting with a gradient of ACN (5-95%) in 0.2% ammonia buffer to afford **27** (78 mg, 67%). <sup>1</sup>H NMR (400 MHz, CDCl<sub>3</sub>) δ 7.33 – 7.23 (m, 2H), 6.92 – 6.85 (m, 2H), 4.94 (d, *J* = 6.7 Hz, 2H), 4.57 (d, *J* = 6.7 Hz, 2H), 3.97 (s, 2H), 3.81 (s, 3H), 2.59 (t, *J* = 7.2 Hz, 2H), 2.26 – 2.17 (m, 2H), 1.76 – 1.65 (m, 2H). HRMS calcd for C<sub>14</sub>H<sub>20</sub>NO<sub>2</sub><sup>+</sup>, [M + H]<sup>+</sup>, 234.1494; found 234.1497.

**(1-(4-methoxybenzyl)pyrrolidine-2,2-diyl)dimethanol (28).**

**27** (40 mg, 0.17 mmol) and  $\text{BF}_3 \cdot \text{OET}_2$  (0.065 mL, 0.51 mmol) were mixed in DCM (1 mL) to give a tan solution. The reaction was stirred at rt over weekend.  $\text{NaHCO}_3$  (sat. 3 ml) and DCM:MeOH 90:10 (3 ml) were added and the mixture stirred at rt for 15 min, filtered through a phase separator and evaporated. The compound was purified by preparative HPLC on a XBridge C18 column (10  $\mu\text{m}$  250x19 ID mm) using a gradient of 15-60% ACN in  $\text{H}_2\text{O}/\text{ACN}/\text{NH}_3$  95/5/0.2 buffer over 20 min with a flow of 19 mL/min. The compounds were detected by UV at 235nm to afford **28** (3 mg, 7%).  $^1\text{H}$  NMR (400 MHz, MeOD)  $\delta$  7.20 (d,  $J = 8.6$  Hz, 2H), 6.84 (d,  $J = 8.6$  Hz, 2H), 3.78-3.74 (m, 5H), 3.57 (s, 3H), 2.71 (t,  $J = 6.7$  Hz, 2H), 1.91-1.84 (m, 2H), 1.73-1.63 (m, 2H). HRMS calcd for  $\text{C}_{14}\text{H}_{22}\text{NO}_3^+$ ,  $[\text{M} + \text{H}]^+$ , 252.1599; found 252.1617.

**(5-(4-methoxyphenyl)-1,3,4-oxadiazol-2-yl)(3-(4-(((3-methyloxetan-3-yl)methoxy)methyl)phenoxy)azetidin-1-yl)methanone (36).**

*(3-methyloxetan-3-yl)methyl methanesulfonate (52)*. (3-Methyloxetan-3-yl)methanol (225 mg, 2.20 mmol) and TEA (0.461 mL, 3.30 mmol) were in mixed DCM (5 mL) to give a colorless solution.  $\text{MsCl}$  (0.206 mL, 2.64 mmol) was added dropwise and the reaction stirred at rt overnight. Water (5 mL) was added, the mixture stirred, filtered through a phase separator and evaporated to give **52** (320 mg, 81%).  $^1\text{H}$  NMR (400 MHz,  $\text{CDCl}_3$ )  $\delta$  1.39 (s, 3H), 3.07 (s, 3H), 4.32 (s, 2H), 4.43 (d,  $J = 6.3$  Hz, 2H), 4.51 (d,  $J = 6.3$  Hz, 2H).

*3-(((4-(benzyloxy)benzyl)oxy)methyl)-3-methyloxetane (53)*. (4-(Benzyloxy)phenyl)methanol (357 mg, 1.66 mmol) was dissolved in DMF (5 mL) and the mixture was cooled in an ice-bath.  $\text{NaH}$  (73.2 mg, 1.83 mmol) was added and the mixture was stirred from  $0^\circ\text{C}$  to rt for 45 min. The mixture was cooled again in ice-bath and **52** (300 mg, 1.66 mmol) in DMF (4 mL) was added

1  
2  
3 dropwise and the reaction stirred at rt overnight. Water (30 mL) and EtOAc (40 mL) were added,  
4  
5 the mixture stirred and the phases separated. The organic phase was washed with water (3x),  
6  
7 filtered through a phase separator and evaporated. The residue was purified by automated flash  
8  
9 chromatography on a 25g Si column using a gradient from 0% to 20% of EtOAc in heptane over  
10  
11 20CV. The product was collected using the wavelength 275nm to give **53** (110mg, 22%). <sup>1</sup>H  
12  
13 NMR (400 MHz, CDCl<sub>3</sub>) δ 7.3 – 7.49 (m, 5H), 7.23 – 7.29 (m, 2H), 6.93 – 7.01 (m, 2H), 5.07 (s,  
14  
15 2H), 4.47 – 4.55 (m, 4H), 4.36 (d, *J* = 5.7 Hz, 2H), 3.50 (s, 2H), 1.33 (s, 3H).  
16  
17  
18  
19

20  
21 *4-(((3-methyloxetan-3-yl)methoxy)methyl)phenol (54)*. **53** (110 mg, 0.37 mmol) and Pd-C (78  
22  
23 mg, 0.04 mmol) were mixed in MeOH (2 mL) to give a suspension. The mixture was stirred  
24  
25 under H<sub>2</sub>, 2 bars, at rt for 1 h, then filtered through a pad of celite with more MeOH and  
26  
27 evaporated to give **54** (62 mg, 81%). LCMS (ES-) *m/z* [M - H]<sup>-</sup>: 207.1.  
28  
29

30  
31 *(5-(4-methoxyphenyl)-1,3,4-oxadiazol-2-yl)(3-(4-(((3-methyloxetan-3-yl)methoxy)methyl)phenoxy)azetid-1-yl)methanone (36)*. **54** (40 mg, 0.19 mmol), 1-(5-(4-  
32  
33 methoxyphenyl)-1,3,4-oxadiazole-2-carbonyl)azetid-3-yl methanesulfonate (67.9 mg, 0.19  
34  
35 mmol) and cesium carbonate (75 mg, 0.23 mmol) were mixed in DMA (1 mL) and the reaction  
36  
37 stirred at 90°C for 2 days. DCM (3 mL) and NaHCO<sub>3</sub> (aq 3 mL) were added, the mixture stirred,  
38  
39 filtered through a phase separator and evaporated. The residue was purified by preparative HPLC  
40  
41 eluting with a gradient of ACN (5-95%) in 0.2% ammonia buffer to afford **36** (5.4 mg, 6%). <sup>1</sup>H  
42  
43 NMR (400 MHz, CDCl<sub>3</sub>) δ 8.17 – 8.04 (m, 2H), 7.33 – 7.28 (m, 2H), 7.06 – 7.00 (m, 2H), 6.80 –  
44  
45 6.75 (m, 2H), 5.18 – 5.05 (m, 2H), 4.80 – 4.73 (m, 1H), 4.70 – 4.62 (m, 1H), 4.56 – 4.49 (m,  
46  
47 4H), 4.41 – 4.30 (m, 3H), 3.90 (s, 3H), 3.52 (s, 2H), 1.34 (s, 3H). HRMS calcd for C<sub>25</sub>H<sub>28</sub>N<sub>3</sub>O<sub>6</sub><sup>+</sup>,  
48  
49 [M + H]<sup>+</sup>, 466.1978; found 466.1983.  
50  
51  
52  
53  
54  
55  
56  
57  
58  
59  
60

### ***In vitro* enzyme assays and metabolite identification**

The contribution of different liver enzymes to the metabolism of all compounds was monitored in HLM, HLC or human hepatocytes in the presence or absence of selective inhibitors as described previously,<sup>20</sup> except without progabide.

Incubation mixtures were analyzed by ultra-high performance liquid chromatography/quadrupole time-of-flight mass spectrometry (UHPLC-QTOF-MS) as described previously<sup>20</sup> utilizing a Xevo® G2-S Q-TOF mass spectrometer (Waters, Milford, USA) for compounds in Table 1, or a Synapt G2 Q-TOF (Waters) for compounds in Tables 2, 3 and 4. Data were processed with MetaboLynx V4.1 (Waters). MS and MS<sup>E</sup> spectra were compared between the parent compound and metabolites to identify metabolite structures and site(s) of modification in the substrate molecule. Peak areas were used for the relative quantification of diol metabolites in HLM incubations without NADPH (reported in Tables 1-4), by calculating:

$$Relative\ diol\ \% = \frac{Area_{diol}}{Area_{diol} + Area_{parent}} \times 100$$

For incubations with inhibitors (or those lacking NADPH), relative diol levels were expressed as a percentage of the corresponding peak areas in control incubations with vehicle and NADPH.

### **Computational Methods**

The homology model of human mEH was generated and docking runs were performed, using the highly flexible and transparent homology modelling engine in the MOE software.<sup>41</sup> The homology modelling is based on the atomic coordinates from the fully resolved residues in the template structure of the juvenile hormone EH from the silkworm *Bombyx mori* (PDB ID:

1  
2  
3 4QLA). The structure of the homology model is shown in Figure S2 together with superposed  
4  
5 template structure, a structure model of bacterial EH from *Streptomyces carzinostaticus* (PDB  
6  
7 ID: 4I19), and a complex with fungal EH from *Asperillus niger* EH and the enzyme inhibitor  
8  
9 valpromide (2-propylpentanamide) (PDB ID: 3G0I). The superimposed valpromide structure was  
10  
11 used in the homology modelling procedure together with the template structure with the purpose  
12  
13 of building a model which can accommodate a ligand in a binding pose suitable for enzyme  
14  
15 catalysis. The corresponding sequence alignment and sequence similarity analysis are shown in  
16  
17 Figure S2.  
18  
19

20  
21 The docking of potential substrates from the two series was performed in the MOE software by  
22  
23 gradually building the ligand in the binding site. The ligand was guided towards a pose where the  
24  
25 oxetane oxygen was oriented in an optimal position for catalysis with a two-hydrogen bond  
26  
27 interaction with the two tyrosine residues in the catalytic site (Y299 & Y374 with corresponding  
28  
29 alignment positions 278 & 353 in the sequence alignment in Figure S3a). During this process,  
30  
31 conformational relaxation of the ligand was achieved by restricted energy minimizations  
32  
33 allowing for induced fit of the hydrogen-bonding residues (Y299 & Y374). The Amber v10 force  
34  
35 field with Amber charges for the protein and Extended Hückel treatment and AM1-BCC charges  
36  
37 of the ligands were used for energy minimization steps in both homology model generation and  
38  
39 docking of potential substrates. The dockings were used to validate the homology model and  
40  
41 interpret the degree of product formation observed from experiments in terms of the possibility  
42  
43 for the potential substrates to bind in a pose suitable for catalysis.  
44  
45  
46  
47  
48

49 A set of electronic properties were calculated for oxetane/tetrahydrofuran-containing fragments  
50  
51 which included substitutions affecting reactivity (11 fragments in total were identified in the  
52  
53 dataset) using both semiempirical QM calculations (am1 and pm3) and density functional theory  
54  
55  
56  
57  
58  
59  
60

1  
2  
3 B3LYP/6-31G\* calculations. LUMO energies and partial charges for the oxygen and surrounding  
4  
5 carbons in the oxetane/tetrahydrofuran were calculated with the different methods described  
6  
7 above. LUMO energy calculations using the semiempirical methods were also performed on the  
8  
9 whole molecules.  
10

## 11 12 13 14 ASSOCIATED CONTENT

15  
16  
17 The Supporting Information is available free of charge at the ACS Publications website at

18  
19  
20 DOI:

21  
22  
23 The authors will release the atomic coordinates of the microsomal epoxide hydrolase homology  
24  
25 model upon article publication.  
26

27  
28  
29 Molecular formula strings  
30

## 31 32 33 AUTHOR INFORMATION

### 34 35 36 **Corresponding Author**

37  
38 \* Email: [martin.hayes@astrazeneca.com](mailto:martin.hayes@astrazeneca.com), Cardiovascular, Renal and Metabolism, Innovative  
39  
40 Medicines and Early Development Biotech Unit AstraZeneca, Pepparedsleden 1, Mölndal, 431  
41  
42 83, Sweden. Telephone: +46 (0) 31 776 2004; fax: +46 (0) 31 776 3867.  
43  
44

### 45 46 47 **Present Address**

48  
49 § F.T., Development Science, UCB Biopharma, Chemin du Foriest, B-1420 Braine-l'Alleud,  
50  
51 Belgium.  
52  
53  
54  
55  
56  
57  
58  
59  
60

**ORCID**

Francesca Toselli: 000-0002-1313-7052

Marlene Fredenwall: 0000-0003-0300-1132

Peder Svensson: 0000-0002-4233-5816

Anders Johansson: 0000-0002-1467-6795

Lars Weidolf: 0000-0002-7115-1039

Martin Hayes: 0000-0002-2640-8464

**Author Contributions**

LW, AJ, MAH, PS, XL and FT conceived and designed the experiments. FT performed all *in vitro* experiments and LCMS analysis. PS performed the computational modelling work. MF synthesized additional tool compounds. The manuscript was written and reviewed with contributions from all authors.

**Notes**

The authors declare no competing financial interest.

**ACKNOWLEDGMENT**

We thank Drs Bruce Hammock and Christophe Morisseau (UC Davis), Dr Neal Castagnoli Jr. (Virginia Tech) and Dr Erick Carreira (ETH) for useful discussion. We also thank AstraZeneca chemists from the former MChr1 and 11 $\beta$ -HSD1 projects for the preparation of several compounds used in this project.

## ABBREVIATIONS

ACN, acetonitrile; AO, Aldehyde Oxidase;  $CL_{int}$ , intrinsic clearance; CYP, cytochrome P450; DCM, dichloromethane; DDI, drug-drug interaction; DMA, *N,N*-Dimethylacetamide; DMF, *N,N*-Dimethylformamide; DMSO, dimethyl sulfoxide; EtOAc, ethyl acetate; Hhep, human hepatocytes; HLC, human liver cytosol; HLM, human liver microsomes; HOAc, acetic acid; HRMS, high-resolution mass spectrometry; KTZ, ketoconazole; LUMO, lowest unoccupied molecular orbital; MsCl, Methanesulfonyl chloride; mEH, microsomal epoxide hydrolase; NADPH, Nicotinamide adenine dinucleotide phosphate (reduced form); PDB, protein data bank; PK, pharmacokinetics; QM, quantum mechanical; RT, room temperature; SAR, structure-activity relationship; sEH, soluble epoxide hydrolase; TEA, triethylamine; THF, tetrahydrofuran; TsCl, *p*-Toluenesulfonyl chloride; UHPLC-MS, ultra-high performance liquid chromatography/mass spectrometry; *t*-AUCB, trans-4-[4-(1-adamantylcarbamoylamino)cyclohexyloxy]benzoic acid; VPD, valpromide.

## REFERENCES

- 1) Rendic, S.; Guengerich, F. P. Survey of human oxidoreductases and cytochrome P450 enzymes involved in the metabolism of xenobiotic and natural chemicals. *Chem. Res. Toxicol.* **2015**, *28*, 38-42.
- 2) Zanger U. M.; Schwab M. Cytochrome P450 enzymes in drug metabolism: Regulation of gene expression, enzyme activities, and impact of genetic variation. *Pharmacol. Therapeut.* **2013**, *138*, 103–141.

- 1  
2  
3 3) Garattini, E.; Terao, M. The role of aldehyde oxidase in drug metabolism. *Expert Opin. Drug*  
4  
5 *Metab.* **2012**, *8*, 487-503.  
6  
7  
8 4) Sanoh, S.; Tayama, Y.; Sugihara, K.; Kitamura, S.; Ohta, S. Significance of aldehyde oxidase  
9 during drug development: Effects on drug metabolism, pharmacokinetics, toxicity, and efficacy  
10  
11 *Drug Metab. Pharm.* **2015**, *30*, 52-63.  
12  
13  
14 5) Hutzler, J. M.; Obach, R.S.; Dalvie, D.; Zientek, M.A. Strategies for a comprehensive  
15 understanding of metabolism by aldehyde oxidase. *Expert Opin. Drug Metab. Toxicol.* **2013**, *9*,  
16 153-168.  
17  
18  
19 6) Foti, R. S.; Dalvie, D. K. Cytochrome P450 and non-cytochrome P450 oxidative metabolism:  
20 Contributions to the pharmacokinetics, safety, and efficacy of xenobiotics. *Drug Metab. Dispos.*  
21 **2016**, *44*, 1229-1245.  
22  
23  
24 7) Argikar, U.A.; Potter, P.M.; Hutzler, J. M.; Marathe, P.H. Challenges and opportunities with  
25 non-CYP enzymes aldehyde oxidase, carboxylesterase, and UDP-glucuronosyltransferase: Focus  
26 on reaction phenotyping and prediction of human clearance. *AAPS Journal*, **2016**, *18*, 1391-  
27 1405.  
28  
29  
30 8) Jensen, K.G.; Jacobsen, A-M; Bundgaard, C.; Nilausen, D. Ø.; Thale, Z.; Chandrasena, G.;  
31 Jørgensen, M. Lack of exposure in a first-in-man study due to aldehyde oxidase metabolism:  
32 Investigated by use of <sup>14</sup>C-microdose, humanized mice, monkey pharmacokinetics, and in vitro  
33 methods. *Drug Metab. Dispos.* **2017**, *45*, 68–75.  
34  
35  
36 9) Bull, J.A.; Croft, R.A.; Davis, O.A.; Doran, R.; Morgan, K.F. Oxetanes: recent advances in  
37 synthesis, reactivity, and medicinal chemistry. *Chem. Rev.* **2016**, *116*, 12150–12233.  
38  
39  
40  
41  
42  
43  
44  
45  
46  
47  
48  
49  
50  
51  
52  
53  
54  
55  
56  
57  
58  
59  
60

- 1  
2  
3 10) Carreira, E. M.; Fessard, T. C. Four-membered ring-containing spirocycles: Synthetic  
4 strategies and opportunities. *Chem. Rev.* **2014**, *114*, 8257-8322.  
5  
6  
7  
8  
9 11) McDougall, L.; Draper, E.R.; Beadle, J.D.; Shipman, M.; Raubo, P.; Jamieson,  
10 A.G.; Adams D. J. Enzymatically-stable oxetane-based dipeptide hydrogels. *Chem. Commun.*  
11 **2018**, *54*, 1793-1796.  
12  
13  
14  
15  
16 12) Wuitschik, G.; Carreira, E. M.; Wagner, B.; Fischer, H.; Parrilla, I.; Schuler, F.; Rogers-  
17 Evans, M.; Muller, K. Oxetanes in drug discovery: Structural and synthetic insights. *J. Med.*  
18 *Chem.* **2010**, *53*, 3227-3246.  
19  
20  
21  
22  
23  
24 13) Zheng, Y. J.; Tice, C. M. The utilization of spirocyclic scaffolds in novel drug discovery.  
25 *Expert Opin. Drug Discov.* **2016**, *11*, 831-834.  
26  
27  
28  
29 14) Stepan, A. F.; Karki, K.; McDonald, W. S.; Dorff, P. H.; Dutra, J. K.; DiRico, K. J.; Won,  
30 A.; Subramanyam, C.; Efremov, I. V.; O'Donnell, C. J.; Nolan, C. E.; Becker, S. L.; Pustilnik, L.  
31 R.; Sneed, B.; Sun, H.; Lu, Y.; Robshaw, A. E.; Riddell, D.; O'Sullivan, T. J.; Sibley, E.;  
32 Capetta, S.; Atchison, K.; Hallgren, A. J.; Miller, E.; Wood, A.; Obach, R. S. Metabolism-  
33 directed design of oxetane-containing arylsulfonamide derivatives as  $\gamma$ -secretase inhibitors. *J.*  
34 *Med. Chem.* **2011**, *54*, 7772-7783.  
35  
36  
37  
38  
39 15) Lu, H.; Yang, T.; Xu, Z.; Lin, X.; Ding, Q.; Zhang, Y.; Cai, X.; Dong, K.; Gong, S.; Zhang,  
40 W.; Patel, M.; Copley, R. C. B.; Xiang, J.; Guan, X.; Wren, P.; Ren, F. Discovery of novel 1-  
41 cyclopentenyl-3-phenylureas as selective, brain penetrant, and orally bioavailable CXCR2  
42 antagonists. *J. Med. Chem.* **2018**, *61*, 2518-2532.  
43  
44  
45  
46  
47  
48  
49  
50  
51  
52  
53  
54  
55  
56  
57  
58  
59  
60

1  
2  
3 16) Crawford, J. J.; Johnson, A. R.; Misner, D. L.; Belmont, L. D.; Castanedo, G.; Choy, R.;  
4  
5 Coraggio, M.; Dong, L.; Eigenbrot, C.; Erickson, R.; Ghilardi, N.; Hau, J.; Katewa, A.; Kohli, P.  
6  
7 B.; Lee, W.; Lubach, J. W.; McKenzie, B. S.; Ortwine, D. F.; Schutt, L.; Tay, S.; Wei, B.; Reif,  
8  
9 K.; Liu, L.; Wong, H.; Young, W. B. Discovery of GDC-0853: A potent, selective, and  
10  
11 noncovalent Bruton's Tyrosine Kinase inhibitor in early clinical development. *J. Med. Chem.*  
12  
13 **2018**, *61*, 2227-2245.  
14  
15

16  
17 17) Ouvry, G.; Atrux-Tallau, N.; Bihl, F.; Bondu, A.; Bouix-Peter, C.; Carlavan, I.; Christin, O;  
18  
19 Cuadrado, M-J.; Defoin-Platel, C.; Deret, S.; Duvert, D.; Feret, C.; Forissier, M.; Fournier, J-  
20  
21 F.; Froude, D.; Hacini-Rachinel, F.; Harris, C. S.; Hervouet, C.; Huguet, H.; Lafitte, G.; Luzy, A-  
22  
23 P.; Musicki, B.; Orfila, D.; Ozello, B.; Pascau, C.; Pascau, J.; Parnet, V.; Peluchon, G.; Pierre,  
24  
25 R.; Piwnica, D.; Raffin, C.; Rossio, P.; Spiesse, D.; Taquet, N.; Thoreau, E.; Vatinel, R.; Vial, E.;  
26  
27 Hennequin, L. F. Discovery and characterization of CD12681, a potent ROR $\gamma$  inverse agonist,  
28  
29 preclinical candidate for the topical treatment of psoriasis. *ChemMedChem*. **2018**, *13*, 321-337.  
30  
31  
32  
33

34  
35 18) Cheong, J. E.; Zaffagni, M.; Chung, I.; Xu, Y.; Wang, Y.; Jernigan, F. E.; Zetter, B. R.; Sun,  
36  
37 L. Synthesis and anticancer activity of novel water soluble benzimidazole carbamates. *Eur. J.*  
38  
39 *Med. Chem.* **2018**, *144*, 372-385.  
40  
41

42  
43 19) Geary, G. C.; Nortcliffe, A.; Pearce, C. A.; Hamza, D.; Jones, G.; Moody, C. J. Densely  
44  
45 functionalised spirocyclic oxetane-piperidine scaffolds for drug discovery. *Bioorg. Med. Chem.*  
46  
47 **2018**, *26*, 791-797.  
48  
49

50  
51 20) Bezençon, O.; Heidmann, B.; Siegrist, R.; Stamm, S.; Richard, S.; Pozzi, D.; Corminboeuf,  
52  
53 O.; Roch, C.; Kessler, M.; Ertel, E. A.; Reymond, I.; Pfeifer, T.; de Kanter, R.; Toeroek-  
54  
55 Schafroth, M.; Moccia, L. G.; Mawet, J.; Moon, R.; Rey, M.; Capeleto, B.; Fournier, E.  
56  
57  
58  
59  
60

1  
2  
3 Discovery of a potent, selective T-type calcium channel blocker as a drug candidate for the  
4 treatment of generalized epilepsies. *J. Med. Chem.* **2017**, *60*, 9769-9789.

5  
6  
7  
8 21) Johansson, A.; Lofberg, C.; Antonsson, M.; von Unge, S.; Hayes, M. A.; Judkins, R.; Ploj,  
9 K.; Benthem, L.; Linden, D.; Brodin, P.; Wennerberg, M.; Fredenwall, M.; Li, L.; Persson, J.;  
10 Bergman, R.; Pettersen, A.; Gennemark, P.; Hogner, A. Discovery of (3-(4-(2-oxa-6-  
11 azaspiro[3.3]heptan-6-ylmethyl)phenoxy)azetid-1-yl)(5-(4-methoxy phenyl)-1,3,4-oxadiazol-  
12 2-yl)methanone (AZD1979), a melanin concentrating hormone receptor 1 (MCHr1) antagonist  
13 with favorable physicochemical properties. *J. Med. Chem.* **2016**, *59*, 2497-2511.  
14  
15  
16  
17  
18  
19  
20  
21  
22

23 22) Li, X. Q.; Hayes, M. A.; Grönberg, G.; Berggren, K.; Castagnoli, N., Jr.; Weidolf, L.  
24 Discovery of a novel microsomal epoxide hydrolase-catalyzed hydration of a spiro oxetane.  
25 *Drug Metab. Disp.* **2016**, *44*, 1341-1348.  
26  
27  
28  
29  
30

31 23) Morisseau, C.; Hammock, B. D. Epoxide hydrolases: Mechanisms, inhibitor designs, and  
32 biological roles. *Annu. Rev. Pharmacol. Toxicol.* **2005**, *45*, 311-333.  
33  
34  
35

36 24) Vaclavikova, R.; Hughes, D. J.; Soucek, P. Microsomal epoxide hydrolase 1 (EPHX1):  
37 Gene, structure, function, and role in human disease. *Gene* **2015**, *571*, 1-8.  
38  
39  
40

41 25) Toselli, F.; Fredenwall, M.; Svensson, P.; Li, X.Q.; Johansson, A.; Weidolf, L.; Hayes, M.A.  
42 Oxetane substrates of human microsomal epoxide hydrolase. *Drug Metab. Disp.* **2017**, *45*, 966-  
43 973.  
44  
45  
46  
47  
48

49 26) For revised IUBMB Enzyme Nomenclature for mEH EC 3.3.2.9.,  
50 <https://www.qmul.ac.uk/sbcs/iubmb/enzyme/EC3/3/2/9.html> (accessed April 24, 2019).  
51  
52  
53  
54  
55  
56  
57  
58  
59  
60

- 1  
2  
3 27) Gill, A. L.; Leach, A.; Packer, M.; Scott, J. S.; Sorme, P.; Swales, J. G.; Whittamore, P. R. O.  
4  
5 Preparation of Substituted Pyrimidine-5-carboxamides as 11 $\beta$ HSD1 Inhibitors for Treating  
6  
7 Diabetes and Obesity. *U.S. Pat. Appl. Publ.* 2009, US 20090264401 A1 20091022  
8  
9  
10  
11 28) Scott, J.S.; Gill, A. L.; Godfrey, L.; Groombridge, S. D.; Rees, A.; Revill, J.; Schofield, P.;  
12  
13 Sorme, P.; Stocker, A.; Swales, J. G.; Whittamore, P. R. O. Optimisation of pharmacokinetic  
14  
15 properties in a neutral series of 11 $\beta$ -HSD1 inhibitors. *Bioorg. Med. Chem.*  
16  
17 *Lett.* **2012**, 22(21), 6756-6761.  
18  
19  
20  
21 29) Goldberg, F.W.; Leach, A.G.; Scott, J.S.; Snelson, W.L.; Groombridge, S.D.; Craig, S.D.;  
22  
23 Bennett, S.N.L.; Bodin, C.; Gutierrez, P.M.; Gyte A.C. Free-Wilson and structural approaches to  
24  
25 co-optimizing human and rodent isoform potency for 11 $\beta$ -hydroxysteroid dehydrogenase Type1  
26  
27 (11 $\beta$ -HSD1) Inhibitors. *J. Med. Chem.* **2012**, 55, 10652–10661.  
28  
29  
30  
31 30) Rioux, N.; Duncan, K. W.; Lantz, R. J.; Miao, X.; Chan-Penebre, E.; Moyer, M. P.;  
32  
33 Munchhof, M. J.; Copeland, R. A.; Chesworth, R.; Waters, N. J. Species differences in  
34  
35 metabolism of EPZ015666, an oxetane-containing protein arginine methyltransferase-5  
36  
37 (PRMT5) inhibitor *Xenobiotica*, **2016**, 46, 268-277.  
38  
39  
40  
41 31) Boström, J.; Hogner, A.; Llinàs, A.; Wellner, E.; Plowright, A. T. Oxadiazoles in medicinal  
42  
43 chemistry. *J. Med. Chem.* **2012**, 55, 1817-1830.  
44  
45  
46  
47 32) Zhou, K.; Jia, N.; Hu, C.; Jiang, Y.L.; Yang, J.P.; Chen, Y.; Li, S.; Li, W.F.; Zhou, C.Z.  
48  
49 Crystal structure of juvenile hormone epoxide hydrolase from the silkworm *Bombyx mori*.  
50  
51 *Proteins* **2014**, 82(11), 3224-3229.  
52  
53  
54  
55  
56  
57  
58  
59  
60

- 1  
2  
3 33) Reetz, M.T.; Bocola, M.; Wang, L.W.; Sanchis, J.; Cronin, A.; Arand, M.; Zou,  
4  
5 J.; Archelas, A.; Bottalla, A.L.; Naworyta, A.; Mowbray, S.L. Directed evolution of an  
6  
7 enantioselective epoxide hydrolase: uncovering the source of enantioselectivity at each  
8  
9 evolutionary stage. *J. Am. Chem. Soc.* **2009**, 131(21), 7334-7343.  
10  
11  
12  
13 34) Saenz-Méndez, P.; Katz, A.; Pérez-Kempner, M.L.; Ventura, O.N.; Vázquez, M. Structural  
14  
15 insights into human microsomal epoxide hydrolase by combined homology modeling, molecular  
16  
17 dynamics simulations, and molecular docking calculations. *Proteins* **2017**, 85(4), 720-730.  
18  
19  
20  
21 35) Lewis, D.F.; Lake, B.G.; Bird, M.G. Molecular modelling of human microsomal epoxide  
22  
23 hydrolase (EH) by homology with a fungal (*Aspergillus niger*) EH crystal structure of 1.8 Å  
24  
25 resolution: structure-activity relationships in epoxides inhibiting EH activity. *Toxicol. In*  
26  
27 *Vitro.* **2005**, 19(4), 517-522.  
28  
29  
30  
31 36) Hammock B., personal communication  
32  
33  
34 37) Shao, Y.; Molnar, L. F.; Jung, Y.; Kussmann, J.; Ochsenfeld, C.; Brown, S. T.; Gilbert, A. T.  
35  
36 B.; Slipchenko, L. V.; Levchenko, S. V.; O'Neill, D. P.; DiStasio, R. A., Jr.; Lochan, R. C.;  
37  
38 Wang, T.; Beran, G. J. O.; Besley, N. A.; Herbert, J. M.; Lin, C. Y.; Van Voorhis, T.; Chien, S.  
39  
40 H.; Sodt, A.; Steele, R. P.; Rassolov, V. A.; Maslen, P. E.; Korambath, P. P.; Adamson, R. D.;  
41  
42 Austin, B.; Baker, J.; Byrd, E. F. C.; Dachsel, H.; Doerksen, R. J.; Dreuw, A.; Dunietz, B. D.;  
43  
44 Dutoi, A. D.; Furlani, T. R.; Gwaltney, S. R.; Heyden, A.; Hirata, S.; Hsu, C-P.; Kedziora, G.;  
45  
46 Khalliulin, R. Z.; Klunzinger, P.; Lee, A. M.; Lee, M. S.; Liang, W.; Lotan, I.; Nair, N.; Peters,  
47  
48 B.; Proynov, E. I.; Pieniazek, P. A.; Rhee, Y. M.; Ritchie, J.; Rosta, E.; Sherrill, C. D.;  
49  
50 Simmonett, A. C.; Subotnik, J. E.; Woodcock, H. L., III; Zhang, W.; Bell, A. T.; Chakraborty, A.  
51  
52 K.; Chipman, D. M.; Keil, F. J.; Warshel, A.; Hehre, W. J.; Schaefer, H. F., III; Kong, J.; Krylov,  
53  
54  
55  
56  
57  
58  
59  
60

- 1  
2  
3 A. I.; Gill, P. M. W.; Head-Gordon, M. Advances in methods and algorithms in a modern  
4 quantum chemistry program package. *Phys. Chem. Chem. Phys.* **2006**, *8*, 3172–3191.  
5  
6  
7  
8 38) Crouch, R. D.; Hutzler, J. M.; Daniels, J. S. A novel in vitro allometric scaling methodology  
9 for aldehyde oxidase substrates to enable selection of appropriate species for traditional  
10 allometry. *Xenobiotica*, **2018**, *48*, 219-231.  
11  
12  
13 39) El-Sherbeni, A. A.; El-Kadi, A. O. S. The role of epoxide hydrolases in health and disease.  
14 *Arch. Toxicol.* **2014**, *88*, 2013-2032.  
15  
16  
17 40) Kitteringham, N. R.; Davis, C.; Howard, N.; Pirmohamed, M.; Park, B. K. Interindividual  
18 and interspecies variation in hepatic microsomal epoxide hydrolase activity: studies with cis-  
19 stilbene oxide, carbamazepine 10,11-epoxide and naphthalene. *J. Pharm. Exp. Ther.* **1996**, *278*,  
20 1018-1027.  
21  
22  
23 41) Molecular Operating Environment (MOE), 2016.08. Chemical Computing Group Inc., 1010  
24 Sherbrooke St. West, Suite #910, Montreal, QC, Canada, H3A 2R7. (2016).  
25  
26  
27 42) Dost, J.; Heschel, M.; Stein, J., Preparation of 1,3,4-oxadiazole-2-carboxylic acid  
28 derivatives. *J. Prakt. Chem.* **1985**, 327(1), 109-16.  
29  
30  
31  
32  
33  
34  
35  
36  
37  
38  
39  
40  
41  
42  
43  
44  
45  
46  
47  
48  
49  
50  
51  
52  
53  
54  
55  
56  
57  
58  
59  
60

## Table of Contents Graphical Abstract

